

Principles for designing sustainable and high-strain rate stress wave dissipating materials

Juho Lee,^{1,2,†} Gyeongmin Park,^{3,†} Dongju Lee,^{1,†} Jiyun Shin,¹ Cheol-Hee Ahn,² Jaejun Lee,^{3,*}
Tae Ann Kim^{1,4,5,*}

¹ Solutions to Electromagnetic Interference in Future-mobility Research Center, Korea Institute of Science and Technology, Seoul 02792, Republic of Korea.

² Research Institute of Advanced Materials, Department of Materials and Science Engineering, Seoul National University, Seoul 08826, Republic of Korea

³ Department of Polymer Science and Engineering, Pusan National University, Busan 46241, Republic of Korea

⁴ Soft Hybrid Materials Research Center, Korea Institute of Science and Technology, Seoul 02792, Republic of Korea

⁵ Division of Energy & Environment Technology, KIST School. Korea University of Science and Technology (UST), Seoul 02792, Republic of Korea

Table of Contents

1. General experimental details	1
1.1 Materials	1
1.2 Characterization	1
2. Synthesis of small molecules	3
2.1 Carbodiimide coupling reaction of LA with aliphatic alcohol and amines	3
2.2 Synthesis of LA modified bifunctional crosslinker (BPA-LA)	5
3. Characterization of linear poly(disulfide)s	6
3.1 Photo-initiated polymerization kinetics of other LA derivatives	6
3.2 Synthetic scheme and NMR results for linear poly(disulfide)s	6
3.3 Chemical recycling of linear poly(disulfide)s	9
3.4 Construction of master curves for linear poly(disulfide)s for each polymer	11
4. Laser-induced shock wave test	17
4.1 Sample preparation	17
4.2 Shock wave test experimental set up	17
4.3 The calculation of strain rate and frequency of the high strain rate stress waves	20
5. Poly(hexyl acrylate)s as control	21
5.1 Polymerization procedure and characterization of poly(hexyl acrylate)s (PHA)	21
5.2 Construction of master curves for PHA	22
5.3 Comparison of high-strain stress wave dissipating abilities of PBuLA and PHA	24
6. Characterization of crosslinked poly(disulfide)s	25
6.1 Preparation method	25
6.2 Rheological behaviors of xPBuLA system	26
6.3 Chemical recycling of xPBuLAs	28
6.4 Construction of master curves for xPBuLA series	29
6.5 X-ray scattering data of xPBuLA series	35
6.6 Relationship between relaxation times and decrease in peak pressure	36
7. ¹H, ¹³C spectra of small molecules	37
8. References	42

1. General experimental details

1.1 Materials

DL- α -Lipoic acid (LA, >99%), 1-(3-dimethylaminopropyl)-3-ethylcarbodiimide hydrochloride (EDCI, >98%), 1-butylamine (>99%), hexyl acrylate (>96%), 1,8-diazabicyclo[5.4.0]-7-undecene (DBU, >98%) were purchased from TCI chemicals. 4-(Dimethylamino) pyridine (DMAP, \geq 99%), 1-butanol (99.8%), 1-octylamine (99%), dodecylamine (98%), phenylbis(2,4,6-trimethylbenzoyl) phosphine oxide (BAPOs, 97%), bisphenol A (BPA, \geq 99%) were sourced from Sigma-Aldrich. Dichloromethane (DCM, 99.7%) was obtained from Alfa chemistry. Acetonitrile (MeCN, 99.9%) and sodium silicate solution (water glass Na_2SiO_3) was acquired from Daejung Chemistry. Polydimethylsiloxane (PDMS) (Sylgard 184) and epoxy (resin: KFR-120V, hardener: KFH-163) were purchased from Dow and Kukdo Chem., respectively. Hexyl acrylate was passed through a basic-activated alumina plug before use to remove the inhibitor and the others were used as received.

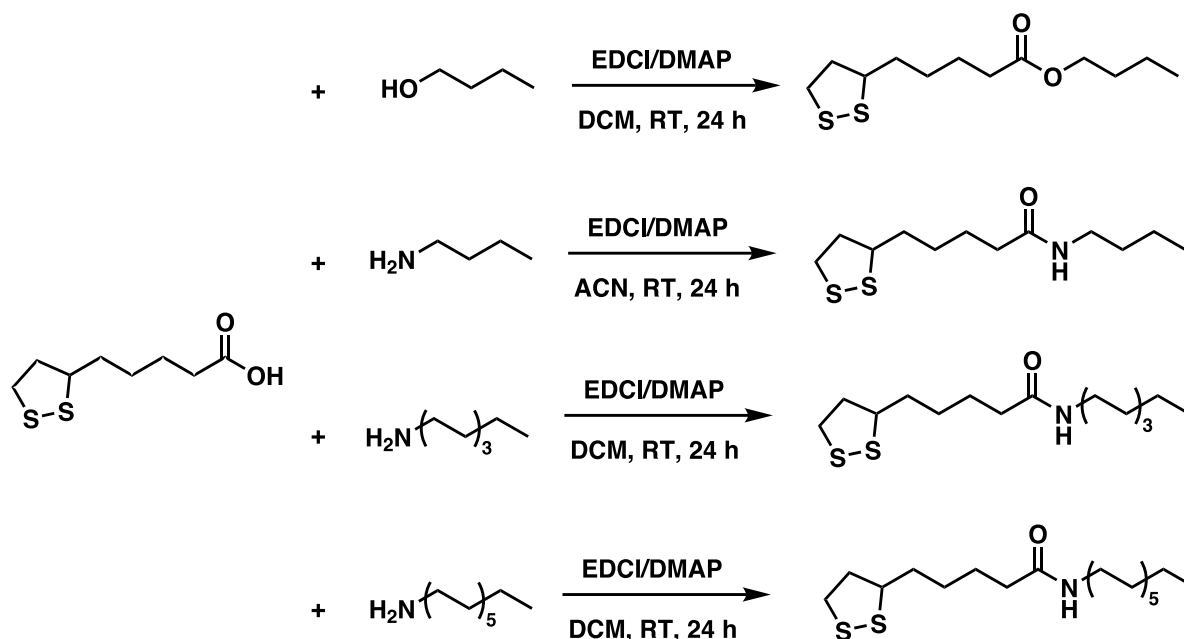
1.2 Characterization

The molecular structures of monomers and confirmation of polymerization were analyzed using nuclear magnetic resonance spectroscopy (NMR, Avance III 400 MHz, Bruker). Gel permeation chromatography (GPC, 1260 Infinity II, Agilent) was performed to determine the molecular weight and dispersity of synthesized linear polymers. Tetrahydrofuran (inhibitor free, HPLC grade, Tedia) was used as an eluent with a flow rate of 1 ml min^{-1} . The molecular weights were calibrated using uniform polystyrene standards. The kinetics of polymerization and curing were observed using a UV/Vis spectrophotometer (V-670, Jasco). UV absorbance spectra were obtained at a scan rate of 400 nm min^{-1} . The microstructures of linear polymers were examined by X-ray diffractometer (XRD, D/MAX 2500/PC, Rigaku) using Cu K α radiation ($\lambda = 1.5406 \text{ \AA}$) and synchrotron SAXS at Beamline 4C of Pohang Accelerator Laboratory. The synchrotron X-ray source had an average photon energy of 16.9 keV with an average beam size of $100 \text{ }\mu\text{m} \times 300 \text{ }\mu\text{m}$ ($V \times H$), and the sample-to-detector distance was 1 m. The scattered photons were recorded using a Rayonix 2D SX 165 CCD detector (Rayonix,

USA) and radially averaged using custom software provided by the beamline. Differential scanning calorimeter (DSC, DSC 4000, Perkin Elmer) was employed to measure the glass transition temperature (T_g) and melting temperature (T_m) of linear polymers. DSC thermograms were obtained from -80 to 90 °C at a heating rate of 10 °C min⁻¹ under a nitrogen atmosphere. The rheological and thermomechanical properties of both linear polymers and crosslinked polymers were examined using a rheometer (MCR 302e, Anton Paar). Dynamic frequency sweep experiments were conducted in the frequency range of 0.1 to 10 Hz at various temperatures to construct master curves through the time-temperature superposition (TTS) method. Temperature sweep tests were carried out from -70 to 100 °C at a heating rate of 5 °C min⁻¹, with a shear strain of 1%. For crosslinked polymers, temperature dependent stress-relaxation tests were performed to calculate the relaxation activation energy (E_a) for the disulfide exchange reaction. A shear strain of 50% was applied to the specimen and the change in modulus was monitored at different temperatures (110, 120, 130 °C for uncatalyzed, and 5, 15, 25 °C for catalyzed system). A cyclic strain sweep test was applied to evaluate the self-healing capabilities of crosslinked polymers. The strain amplitude shifted between 1% and 1500% over four cycles. Except frequency sweep tests, all the measurements were done at a constant frequency of 1 Hz using an 8 mm (diameter) plate geometry.

2. Synthesis of small molecules

2.1 Carbodiimide coupling reaction of LA with aliphatic alcohol and amines



Scheme S1. Synthesis of side chain engineered LA derivatives.

Since the synthetic procedure for each derivative is similar, we have provided a representative synthetic procedure for butyl lipoate (**BuLA**). EDCI (2.56 g, 13.4 mmol, 1.1 equiv.) and DMAP (0.15 g, 1.22 mmol, 0.1 equiv.) were introduced into a round-bottom flask equipped with a magnetic stirring bar, followed by purging the flask with Ar. Subsequently, DCM (30 ml) was added to the flask, and the mixture was stirred for 5 minutes. Afterward, 1-butanol (1.11 ml, 12.1 mmol, 1 equiv.) was introduced into the flask and stirred. Once the solution achieved a transparent state, a solution of LA (3.00 g, 14.5 mmol, 1.2 equiv.) in DCM (30 ml) was injected and stirred for 24 hours at room temperature. Upon completion of the reaction, the product was condensed and purified through column chromatography to yield as a yellowish viscous gel.

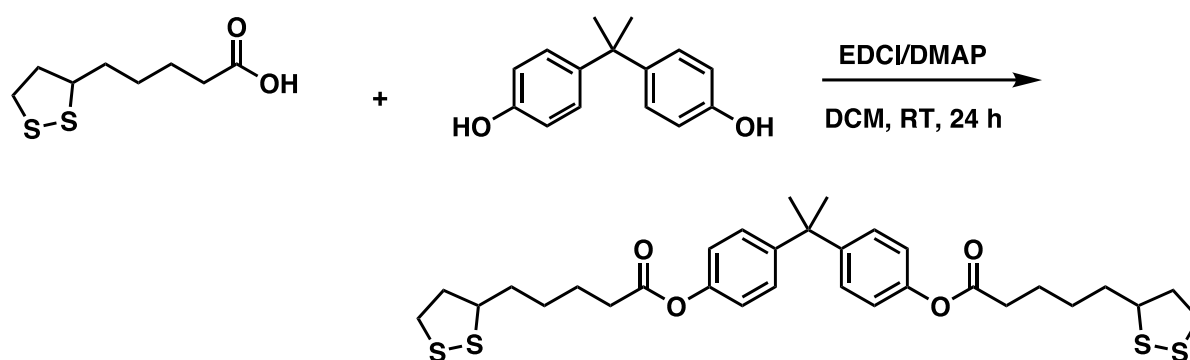
butyl 5-(1,2-dithiolan-3-yl)pentanoate (BuLA): Yield 95%. $^1\text{H NMR}$ (400 MHz, CDCl_3) δ 4.08 (dt, $J = 8.0, 3.7$ Hz, 1H), 3.57 (p, $J = 6.6$ Hz, 0H), 3.24 – 3.06 (m, 1H), 2.46 (dq, $J = 13.0, 6.2$ Hz, 0H), 1.98 – 1.85 (m, 0H), 1.37 (p, $J = 7.6$ Hz, 1H), 1.01 – 0.89 (m, 1H). $^{13}\text{C NMR}$ (101 MHz, CDCl_3) δ 173.65, 64.28, 56.42, 40.29, 38.56, 34.69, 34.19, 30.76, 28.84, 24.80, 19.23, 13.80.

N-butyl-5-(1,2-dithiolan-3-yl)pentanamide (BuLAm): Only for this case, MeCN was used as a solvent. Yield 94%. ^1H NMR (400 MHz, CDCl_3) δ 5.77 (s, 1H), 3.61 – 3.51 (m, 1H), 3.27 – 3.06 (m, 4H), 2.45 (dq, $J = 12.4, 6.2$ Hz, 1H), 2.17 (dd, $J = 8.6, 6.4$ Hz, 2H), 1.90 (dq, $J = 13.5, 6.9$ Hz, 1H), 1.78 – 1.58 (m, 4H), 1.54 – 1.39 (m, 4H), 1.33 (h, $J = 7.3$ Hz, 2H), 0.91 (t, $J = 7.3$ Hz, 3H). ^{13}C NMR (101 MHz, CDCl_3) δ 172.73, 56.50, 40.29, 39.28, 38.53, 36.57, 34.70, 31.79, 29.12, 28.96, 25.55, 20.14, 13.83.

5-(1,2-dithiolan-3-yl)-N-octylpentanamide (OcLAm): Yield 92%. ^1H NMR (400 MHz, CDCl_3) δ 5.69 (s, 1H), 3.60 (p, $J = 6.5$ Hz, 1H), 3.34 – 3.07 (m, 4H), 2.49 (dq, $J = 12.5, 6.2$ Hz, 1H), 2.29 – 2.17 (m, 2H), 1.94 (dq, $J = 13.5, 6.9$ Hz, 1H), 1.72 (dp, $J = 17.3, 7.6$ Hz, 4H), 1.50 (tq, $J = 12.1, 6.7$ Hz, 4H), 1.39 – 1.19 (m, 10H), 0.90 (t, $J = 6.6$ Hz, 3H). ^{13}C NMR (101 MHz, CDCl_3) δ 172.70, 56.51, 40.31, 39.62, 38.54, 36.60, 34.71, 31.86, 29.74, 29.34, 29.28, 28.98, 27.02, 25.56, 22.71, 14.17.

5-(1,2-dithiolan-3-yl)-N-dodecylpentanamide (DdLAm): Yield 86%. ^1H NMR (400 MHz, CDCl_3) δ 5.40 (s, 1H), 3.60 (p, $J = 6.7$ Hz, 1H), 3.30 – 3.09 (m, 4H), 2.48 (dq, $J = 12.4, 6.2$ Hz, 1H), 2.19 (t, $J = 7.5$ Hz, 2H), 1.93 (dq, $J = 13.5, 7.0$ Hz, 1H), 1.70 (tp, $J = 20.2, 6.3$ Hz, 4H), 1.56 – 1.42 (m, 4H), 1.30 (d, $J = 16.1$ Hz, 17H), 0.90 (t, $J = 6.7$ Hz, 3H). ^{13}C NMR (101 MHz, CDCl_3) δ 172.71, 56.53, 40.33, 39.65, 38.56, 36.62, 34.73, 32.00, 29.77, 29.74, 29.72, 29.68, 29.65, 29.43, 29.41, 29.00, 27.04, 25.57, 22.77, 14.21.

2.2 Synthesis of LA modified bifunctional crosslinker (BPA-LA)



Scheme S2. Synthesis of LA-functionalized BPA.

BPA (0.5 g, 2.19 mmol, 1 equiv.), EDCI (1.85 g, 9.65 mmol, 2.2 equiv.), and DMAP (0.11 g, 0.90 mmol, 0.2 equiv.) were charged in a round-bottom flask, followed by purging the flask with Ar. Subsequently, MeCN (30 ml) was added, and the mixture was stirred for 5 minutes. In the next step, a solution of LA (1.13 g, 5.48 mmol, 2.5 equiv.) in MeCN (10 ml) was injected and stirred for 24 hours at room temperature. The solvent was completely removed, and the crude product was purified by column chromatograph to yield light yellow powders (1.22 g, 2.01 mmol, 92 %).

^1H NMR (400 MHz, CDCl_3) δ 7.27 – 7.20 (m, 2H), 7.04 – 6.95 (m, 2H), 3.62 (dq, $J = 8.5, 6.4$ Hz, 1H), 3.26 – 3.11 (m, 2H), 2.59 (t, $J = 7.4$ Hz, 2H), 2.55 – 2.43 (m, 1H), 2.02 – 1.88 (m, 1H), 1.79 (dddd, $J = 23.8, 14.2, 7.8, 4.5$ Hz, 4H), 1.69 (s, 3H), 1.58 (tqd, $J = 18.2, 6.1, 2.0$ Hz, 2H). ^{13}C NMR (101 MHz, CDCl_3) δ 172.11, 148.64, 147.90, 127.90, 120.99, 56.39, 42.55, 40.31, 38.60, 34.69, 34.23, 31.03, 28.79, 24.75.

3. Characterization of linear poly(disulfide)s

3.1 Photo-initiated polymerization kinetics of other LA derivatives

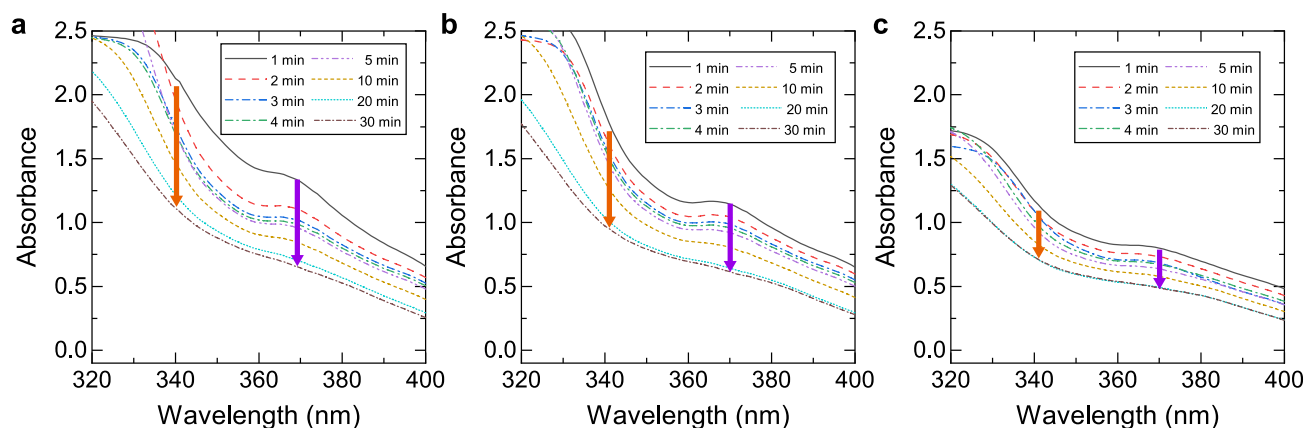


Figure S1. The change in UV-vis absorption spectra of (a) **BuLAm**, (b) **OcLAm**, and (c) **DdLAm**.

3.2 Synthetic scheme and NMR results for linear poly(disulfide)s

The polymerization process is consistent for all monomers. Initially, each monomer (1 g) and the photo-initiator (BAPOs) (3 mol% of monomer) were introduced into a vial. Subsequently, 2 ml of DCM was added, and the mixture was homogeneously blended by vortex mixing. The solution was then heated to 80 °C for 1 hour. Once all the solvents were evaporated, photo-polymerization was carried out using a white lamp (intensity $\approx 70 \text{ mW cm}^{-2}$) for 30 minutes. Each polymer was separated from the monomer using a precipitation solvent (ethanol for **BuLA**, diethyl ether for **BuLAm** and **OcLAm**, methanol for **DdLAm**). The final product was dried under vacuum overnight.

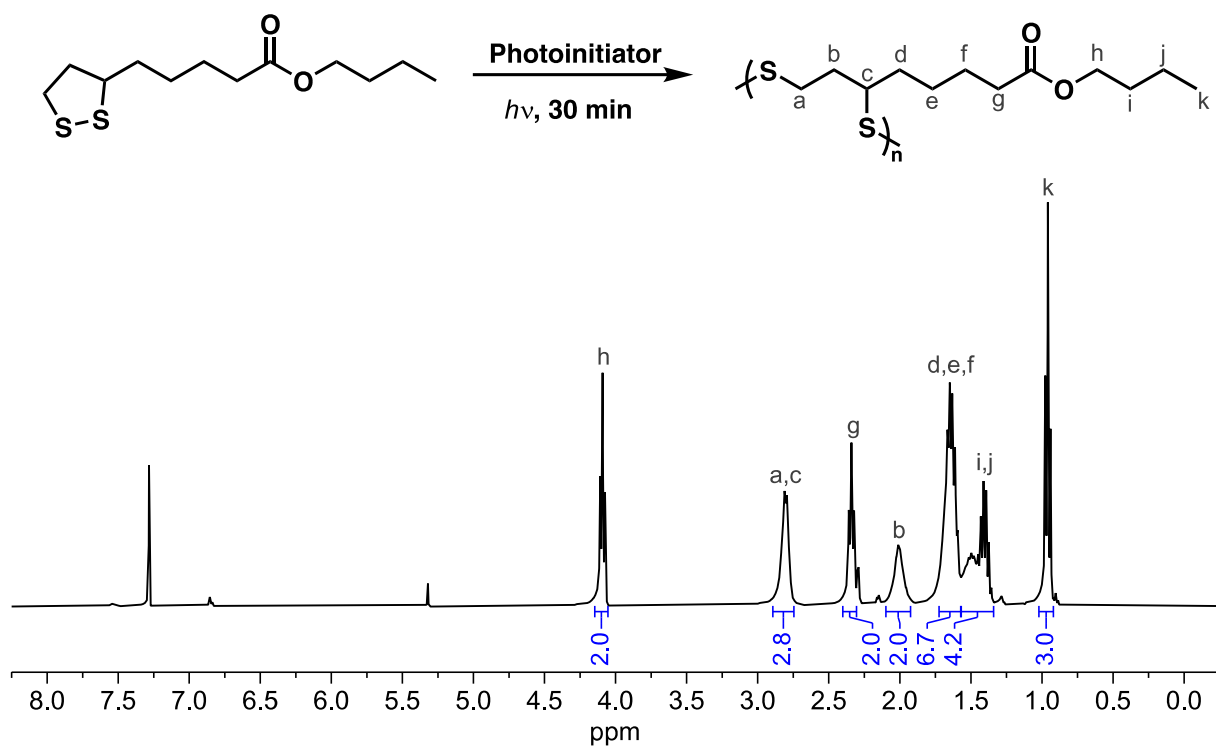


Figure S2. Chemical structure and NMR spectrum of PBuLA.

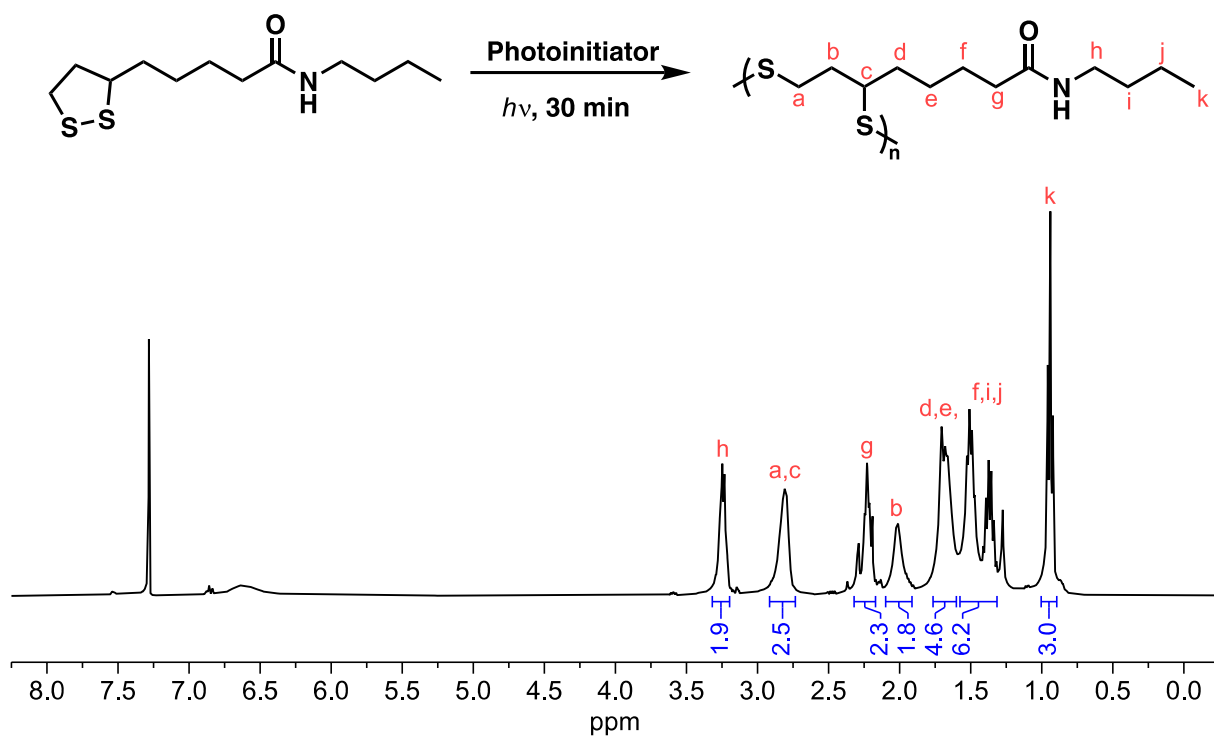


Figure S3. Chemical structure and NMR spectrum of PBuLAm.

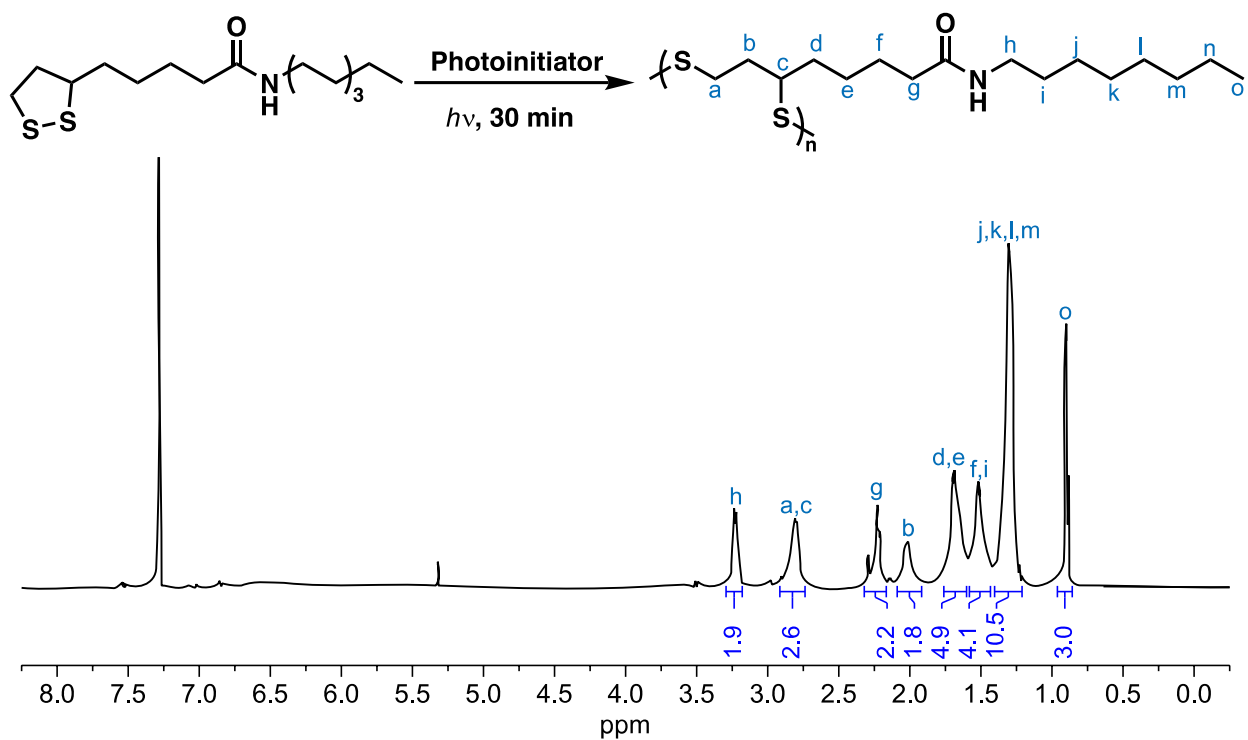


Figure S4. Chemical structure and NMR spectrum of POcLAM.

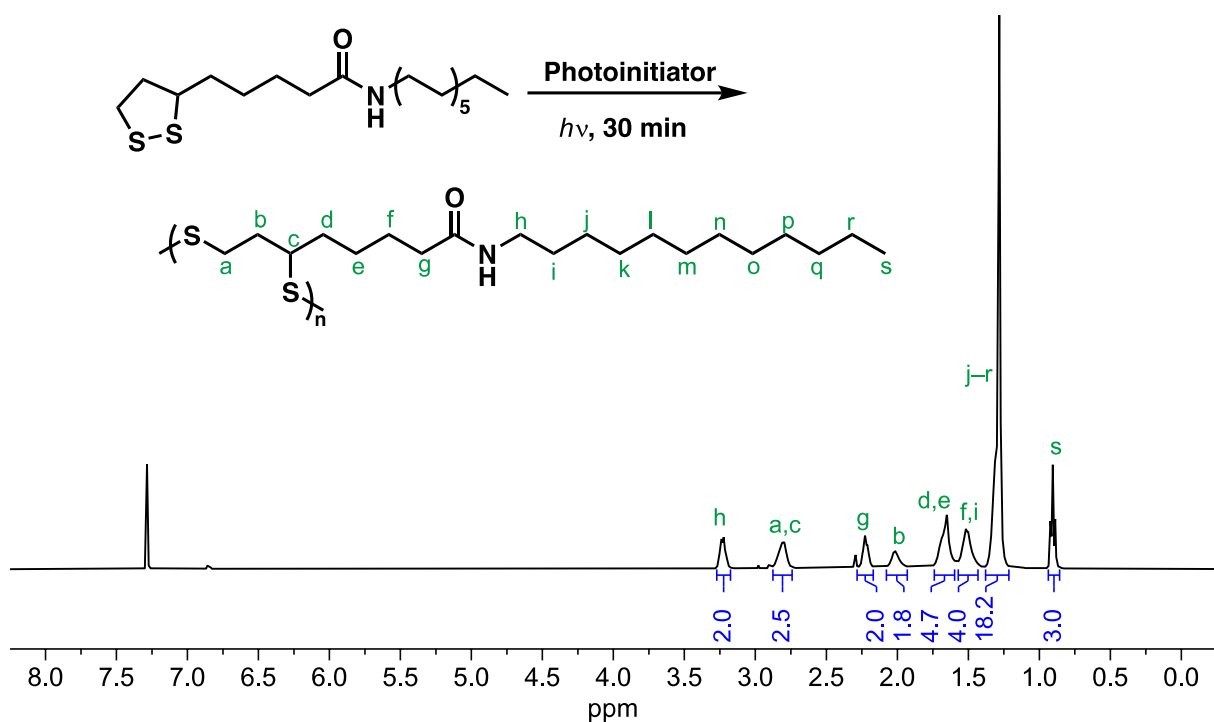


Figure S5. Chemical structure and NMR spectrum of PDDLAM.

3.3 Chemical recycling of linear poly(disulfide)s

The chemical recycling process is consistent for all linear polymers. Initially, each polymer (1 g) was introduced into a round-bottom flask. Subsequently, the flask was purged with Ar and DBU (3 mol% of the polymer) was injected into the reactor. Then, the mixture was dissolved with 60 mL of chloroform and the solution was stirred for 24 hours at room temperature. Upon completion of the reaction (by monitoring TLC), the product was condensed and purified through column chromatography.

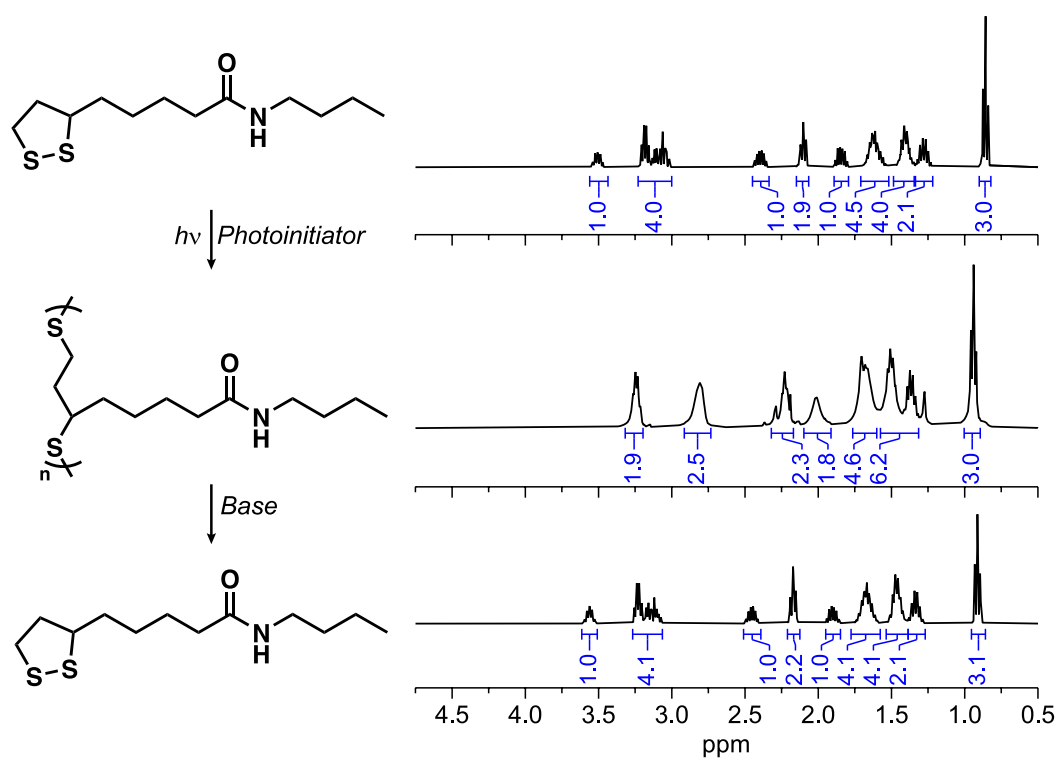


Figure S6. Chemical structure and NMR spectrum of PBUAm.

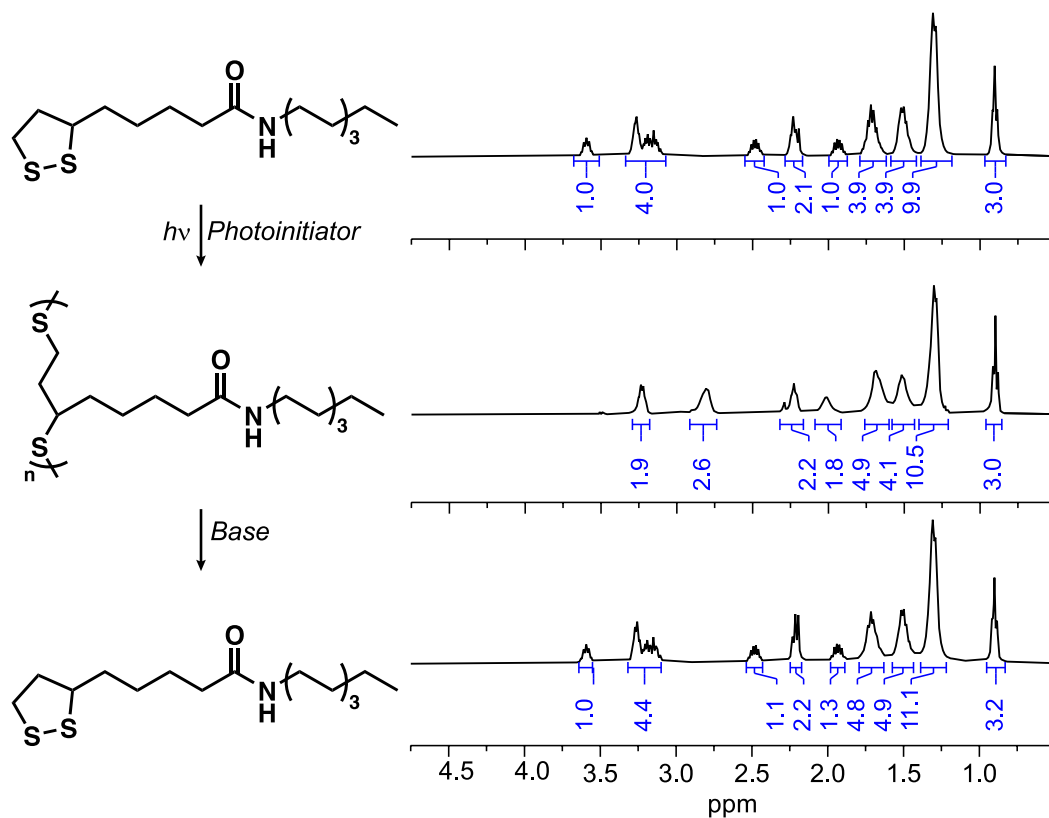


Figure S7. Chemical structure and NMR spectrum of **POcLAM**.

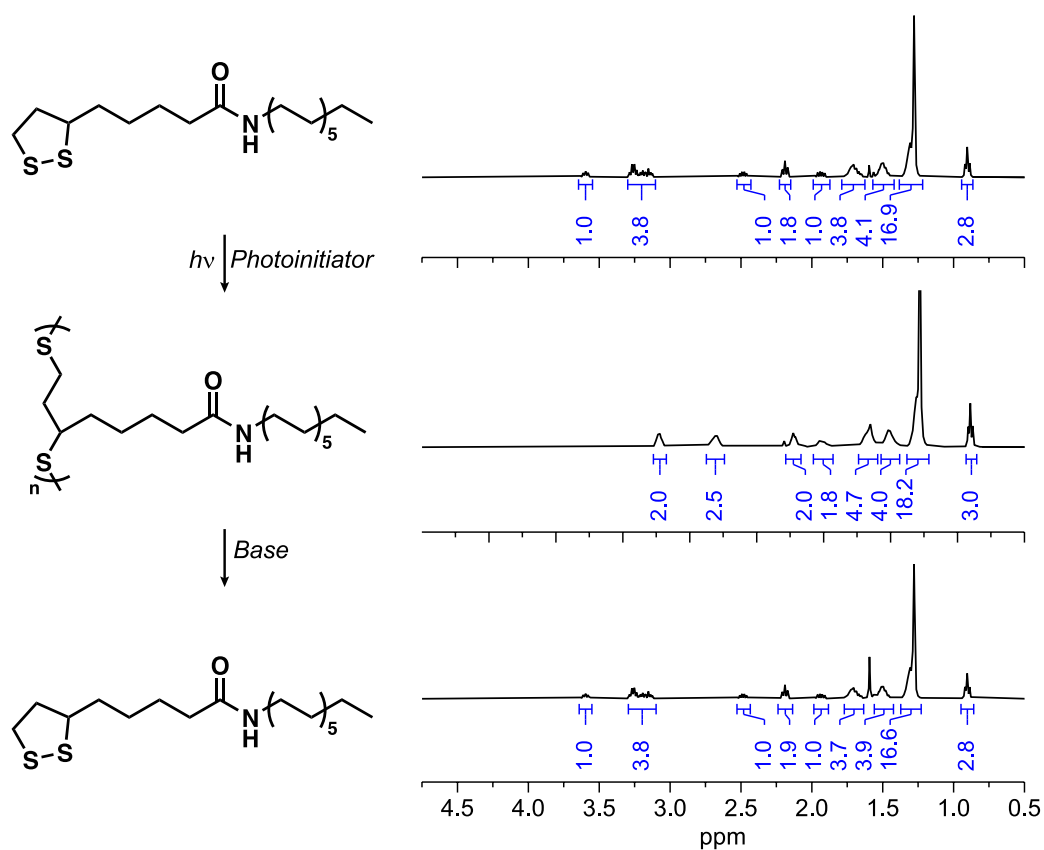


Figure S8. Chemical structure and NMR spectrum of **PDdLAM**.

3.4 Construction of master curves for linear poly(disulfide)s for each polymer.

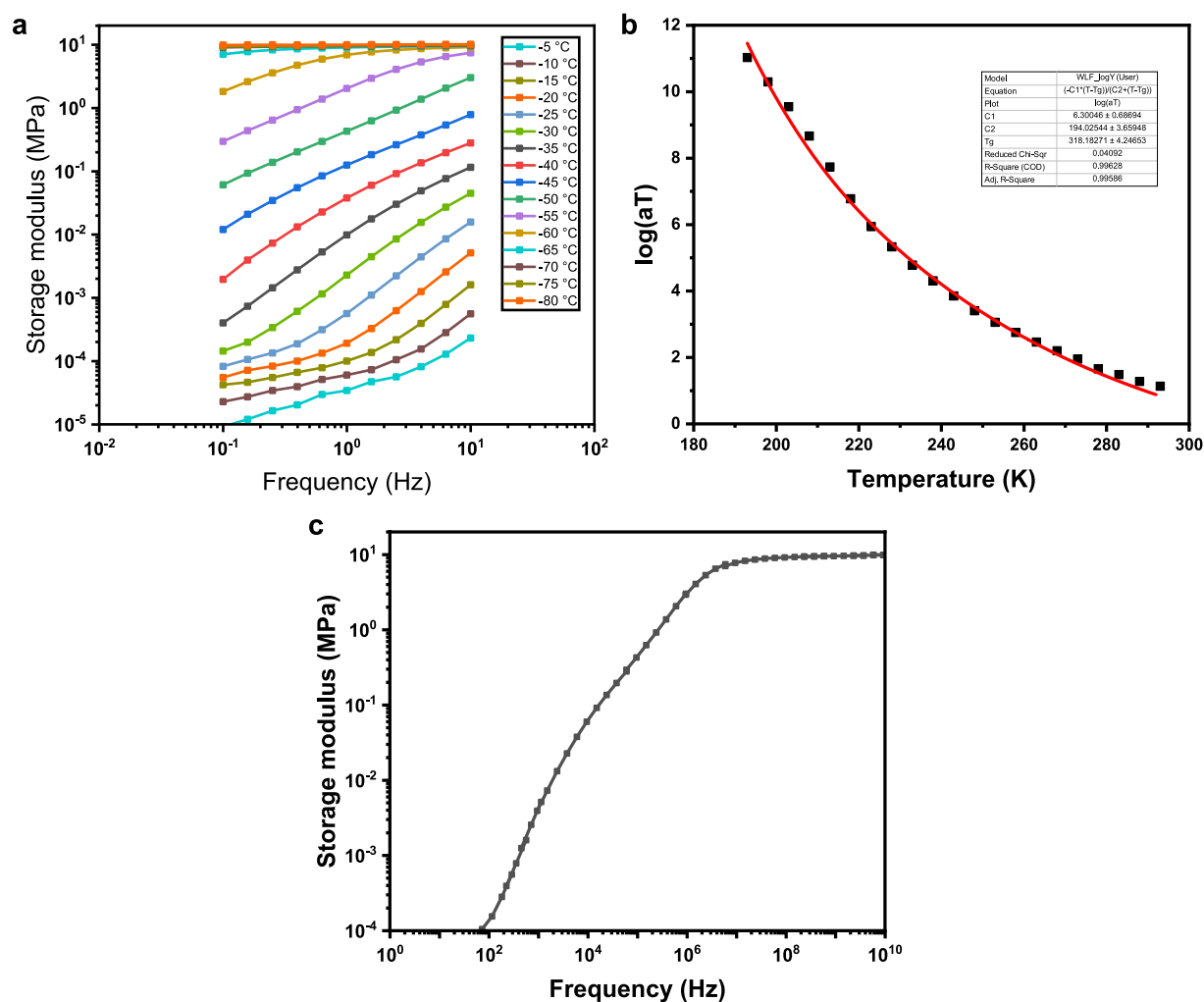


Figure S9. (a) Changes in storage modulus during a frequency sweep (0.1 – 10 Hz) at different temperatures. (b) Time-temperature superposition shift factors (a_T) for **PBuLA** (squares) and WLF fit of the data (red line). (c) Storage modulus master curve of **PBuLA** at a reference temperature of 25 °C.

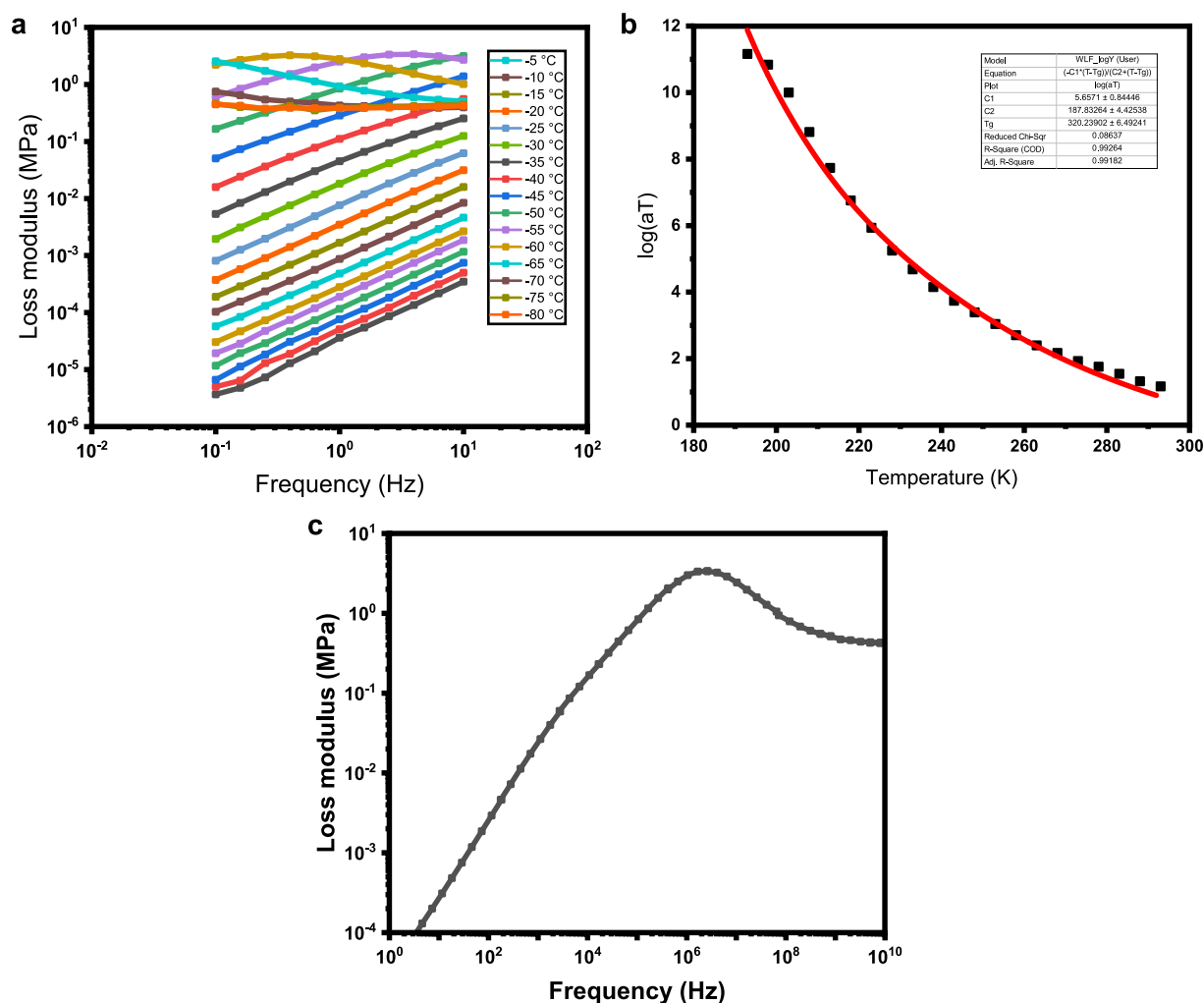


Figure S10. (a) Changes in loss modulus during a frequency sweep (0.1 – 10 Hz) at different temperatures. (b) Time-temperature superposition shift factors (a_T) for **PBuLA** (squares) and WLF fit of the data (red line). (c) Loss modulus master curve of **PBuLA** at a reference temperature of 25 °C.

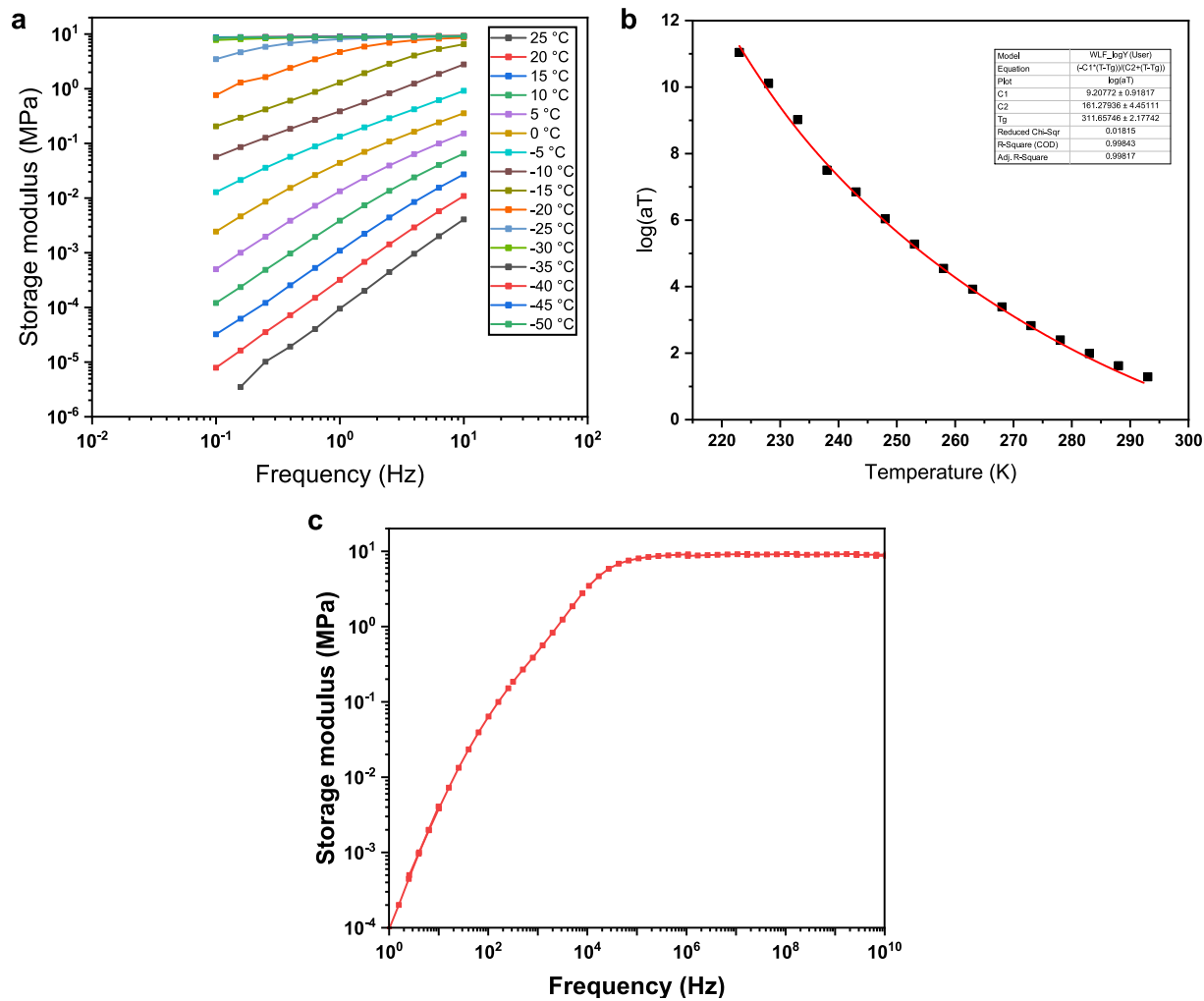


Figure S11. (a) Changes in storage modulus during a frequency sweep (0.1 – 10 Hz) at different temperatures. (b) Time-temperature superposition shift factors (a_T) for **PBuLAm** (squares) and WLF fit of the data (red line). (c) Storage modulus master curve of **PBuLAm** at a reference temperature of 25 °C.

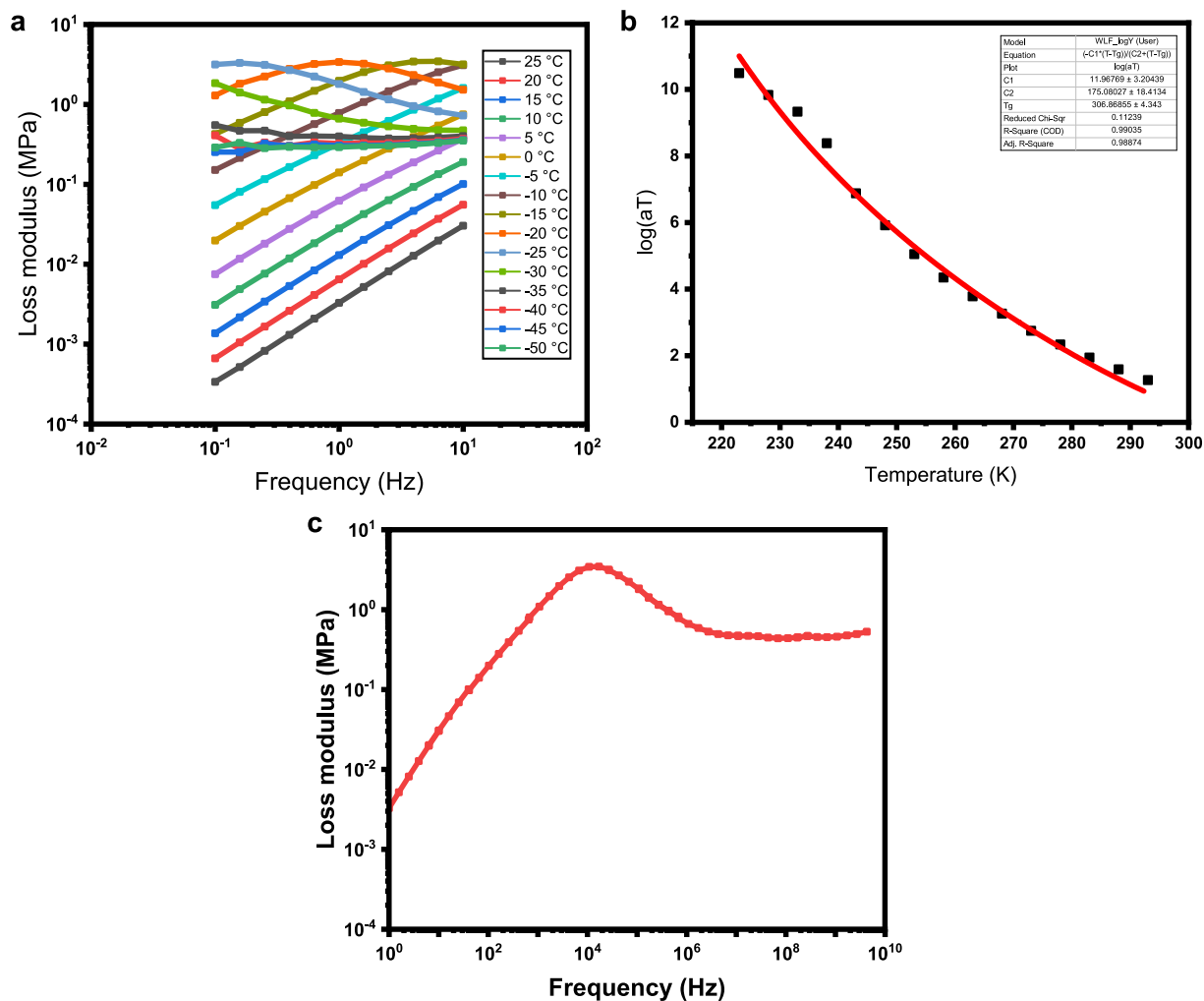


Figure S12. (a) Changes in loss modulus during a frequency sweep (0.1 – 10 Hz) at different temperatures. (b) Time-temperature superposition shift factors (a_T) for **PBuLAm** (squares) and WLF fit of the data (red line). (c) Loss modulus master curve of **PBuLAm** at a reference temperature of 25 °C.

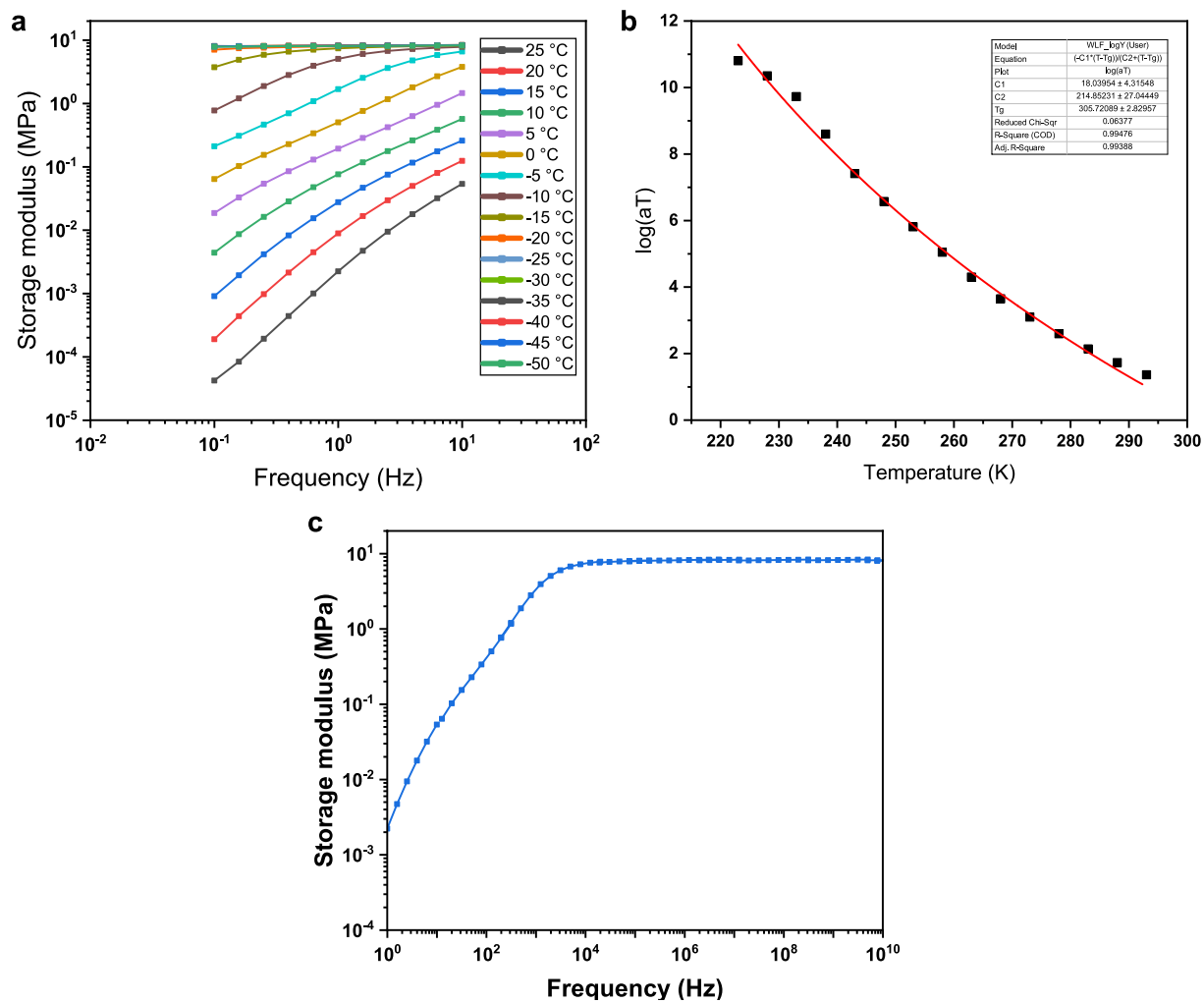


Figure S13. (a) Changes in storage modulus during a frequency sweep (0.1 – 10 Hz) at different temperatures. (b) Time-temperature superposition shift factors (a_T) for **POcLAm** (squares) and WLF fit of the data (red line). (c) Storage modulus master curve of **POcLAm** at a reference temperature of 25 °C.

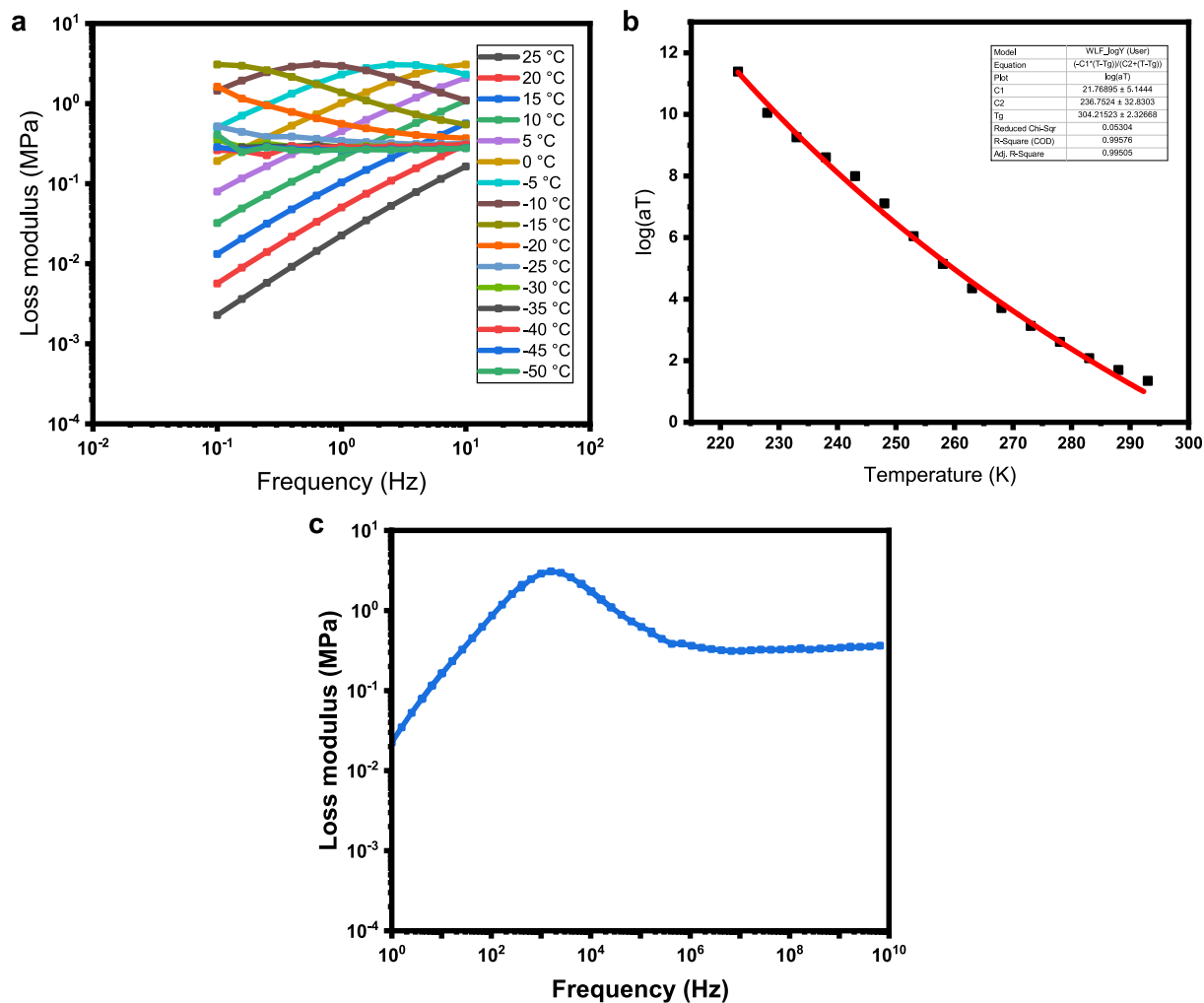


Figure S14. (a) Changes in loss modulus during a frequency sweep (0.1 – 10 Hz) at different temperatures. (b) Time-temperature superposition shift factors (a_T) for **POcLAm** (squares) and WLF fit of the data (red line). (c) Loss modulus master curve of **POcLAm** at a reference temperature of 25 °C.

4. Laser-induced shock wave test

4.1 Sample preparation

Linear and cross-linked poly(disulfides), prepared as described in the manuscript, were sandwiched and stored at room temperature in darkness. To prepare PDMS sample, a base and hardener mixture (Sylgard 184, Dow Chemical) in a 10:1 ratio was sandwiched and cured at 80 °C for 5 hours. The epoxy sample was prepared by mixing a base and hardener (KFR-120V, KFH-163) in a 10:3 ratio, then sandwiched and cured at 85 °C for 2 hours. Both glasses were coated with aluminum (Al) by electron beam deposition, one with 400 nm thickness for energy absorption and the other with 200 nm thickness for reflection. Finally, a 7 μm thick sodium silicate confining layer was deposited by spin coating (ACE-200) of a sodium silicate solution (Na_2SiO_3) on top of the Al absorbing layer for 45 seconds at 1500 rpm.

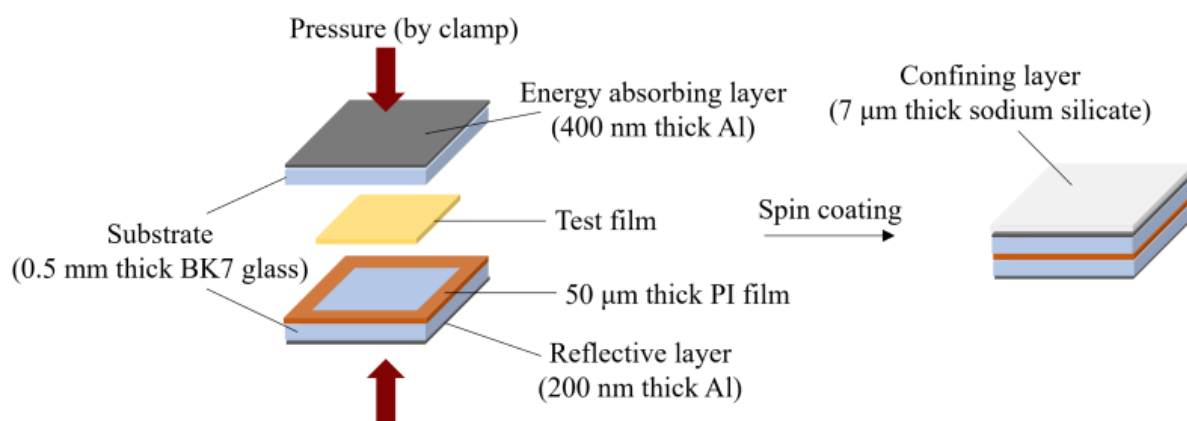


Figure S15. Schematic of a laser-induced shock wave test specimen sandwiched between two glass substrates.

4.2 Shock wave test experimental set up

The application of a laser-induced high strain stress wave to a sandwich specimen configuration and the measurement of stress wave pressure dissipation were described in previous studies (**Figure 2a**).^[1] Q-switched laser pulse ($\lambda = 1064 \text{ nm}$, CNI lasers LPS 1064-L 700 mJ) was directed onto the Al absorbing layer. The rapid expansion of Al, confined by the sodium silicate layer, generated longitudinal stress waves (known as shock waves) that propagated through the glass substrate. After

reflecting at the free surface, the stress wave was loaded on the Al reflective layer and glass substrate, inducing displacement on the Al surface. Using a Michelson interferometer, interferometric measurements on the surface of a 200 nm thick aluminum film quantified the out-of-plane displacement. The interferometer voltage signals, detected by a photodetector connected to a 4 GHz oscilloscope, were then converted into displacement and velocity history following the methodology developed by Wang et al.^[2] The pressure profile, $P(t)$, was obtained from the velocity history using conservation of momentum. $P(t) = \rho_0(U_s(t))U_p(t) = \rho_0(s + cU_p(t))U_p(t)$ (1) where ρ_0 is the initial material density and $U_p(t)$ is the particle velocity obtained from the measurement. Shock velocity, $U_s(t)$, is given by $s + cU_p(t)$, where s and c are fitted parameters from the U_s-U_p Hugoniot relation of the substrate. In this way, we first measured the input peak pressure using the calibration setup without a test film (**Figure S16a**) where the magnitude of the input peak pressure was controlled by tuning the laser intensity and spot size (**Figure S16b**). The input stress wave at 217 mJ mm⁻² input laser fluence corresponds to the peak pressure of ~1 GPa with the duration time of 20 ns (**Figure S16c**). Finally, the stress wave dissipation capability as a percentage of peak pressure dissipation was derived by calculating the pressure reduction from the input average peak pressure.

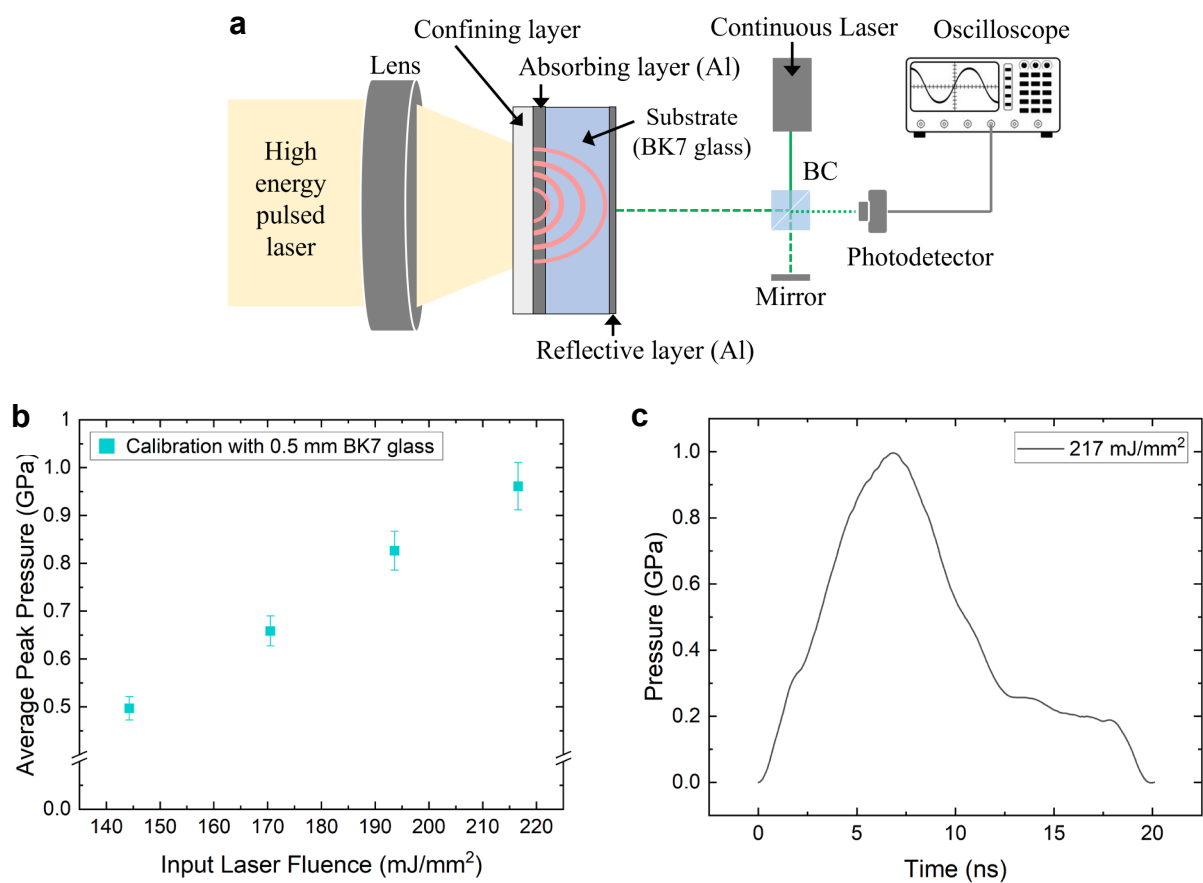


Figure S16. (a) Schematic illustration of the calibration of laser-induced high strain rate stress wave test. (b) Calibration of average peak pressures according to input laser fluence. (c) The representative pressure profile showing that laser-induced stress waves generate a compressive pressure pulse with 20 ns duration at 217 mJ mm^{-2} input laser fluence.

4.3 The calculation of strain rate and frequency of the high strain rate stress waves

In laser-induced shock wave tests, the material strain rate within a typical volume element can be approximated using the equation $\dot{\epsilon} \cong \frac{v}{c\Delta t}$.^[3] Here, v represents the particle velocity generated by the pressure pulse with the duration time Δt in a material element, while a longitudinal wave velocity is represented as c . Nominal strain rates exploited in this study range from $5.5 \times 10^6 \text{ s}^{-1}$ to $9.6 \times 10^6 \text{ s}^{-1}$ since v ranges from 137 to 238 m/s depending on the input laser fluence with the constant values, $\Delta t = 20 \text{ ns}$ and $c = 1240 \text{ m s}^{-1}$.^[4] Finally, the frequencies of the laser-induced high strain rate stress wave were calculated to be between $2.5 \times 10^7 \text{ Hz} \sim 3.6 \times 10^7 \text{ Hz}$, assuming they are the reciprocal of twice the duration time. **(Figure S17b)**

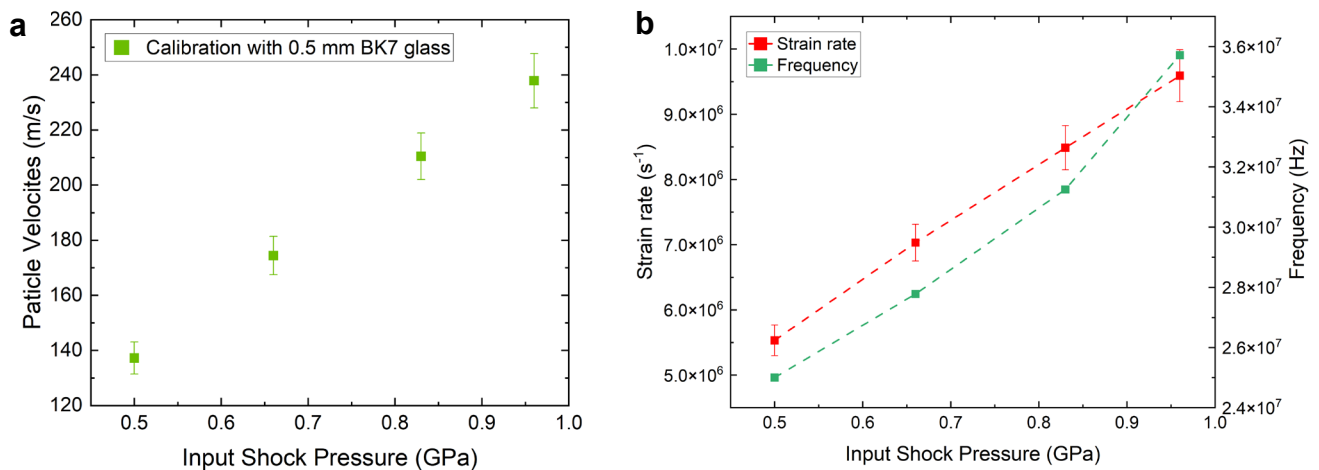


Figure S17. (a) Particle velocity based on input peak pressure, and (b) strain rate and frequency derived from input peak pressure profiles.

5. Poly(hexyl acrylate)s as control

5.1 Polymerization procedure and characterization of poly(hexyl acrylate)s (PHA)

First, hexyl acrylate (3 g) and the photo-initiator (BAPOs) (3 mol% of monomer) were added into a vial. Subsequently, the mixture was homogeneously blended by vortex mixing. Then, the mixture was poured into silicon mold and the photo-polymerization was carried out using a white lamp (intensity $\approx 70 \text{ mW cm}^{-2}$) for 30 minutes. The obtained polymer was used without any precipitation process.

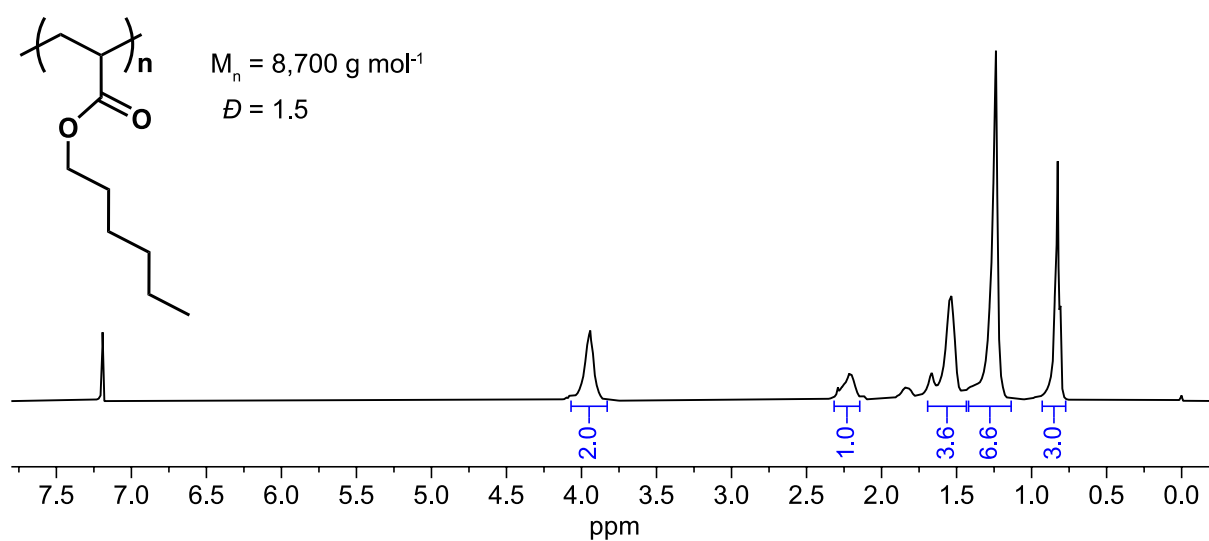


Figure S18. Chemical structure, NMR spectrum, and GPC results of PHA.

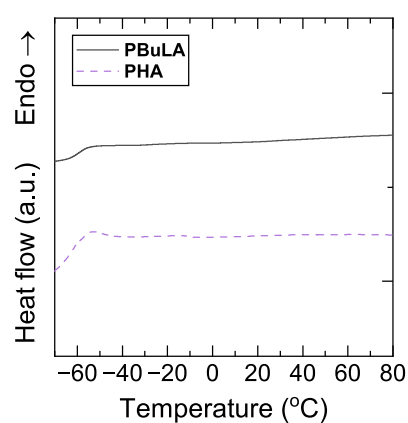


Figure S19. Heat flow thermograms of PBuLA and PHA.

5.2 Construction of master curves for PHA

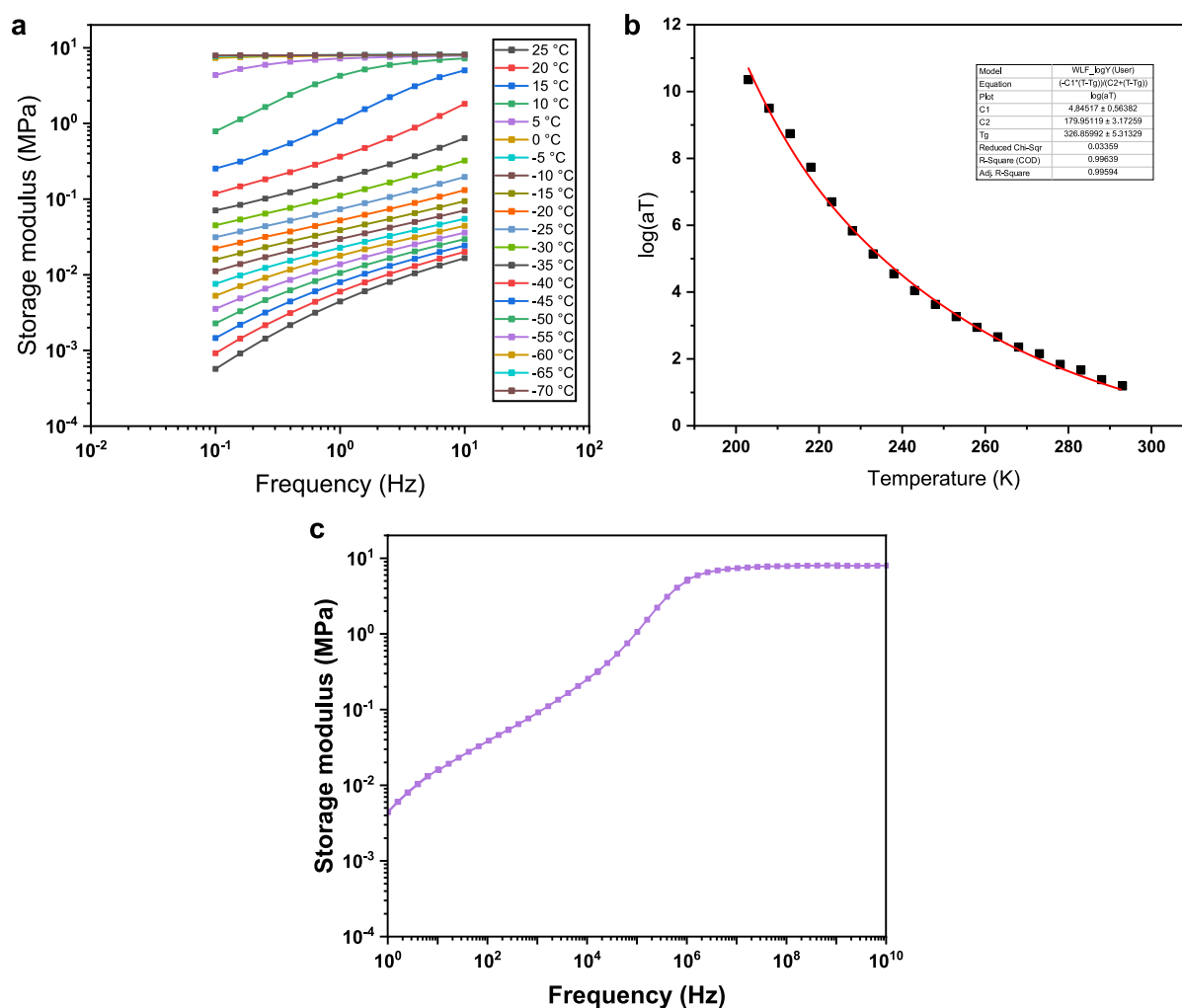


Figure S20. (a) Changes in storage modulus during a frequency sweep (0.1 – 10 Hz) at different temperatures. (b) Time-temperature superposition shift factors (a_T) for **PHA** (squares) and WLF fit of the data (red line). (c) Storage modulus master curve of **PHA** at a reference temperature of 25 °C.

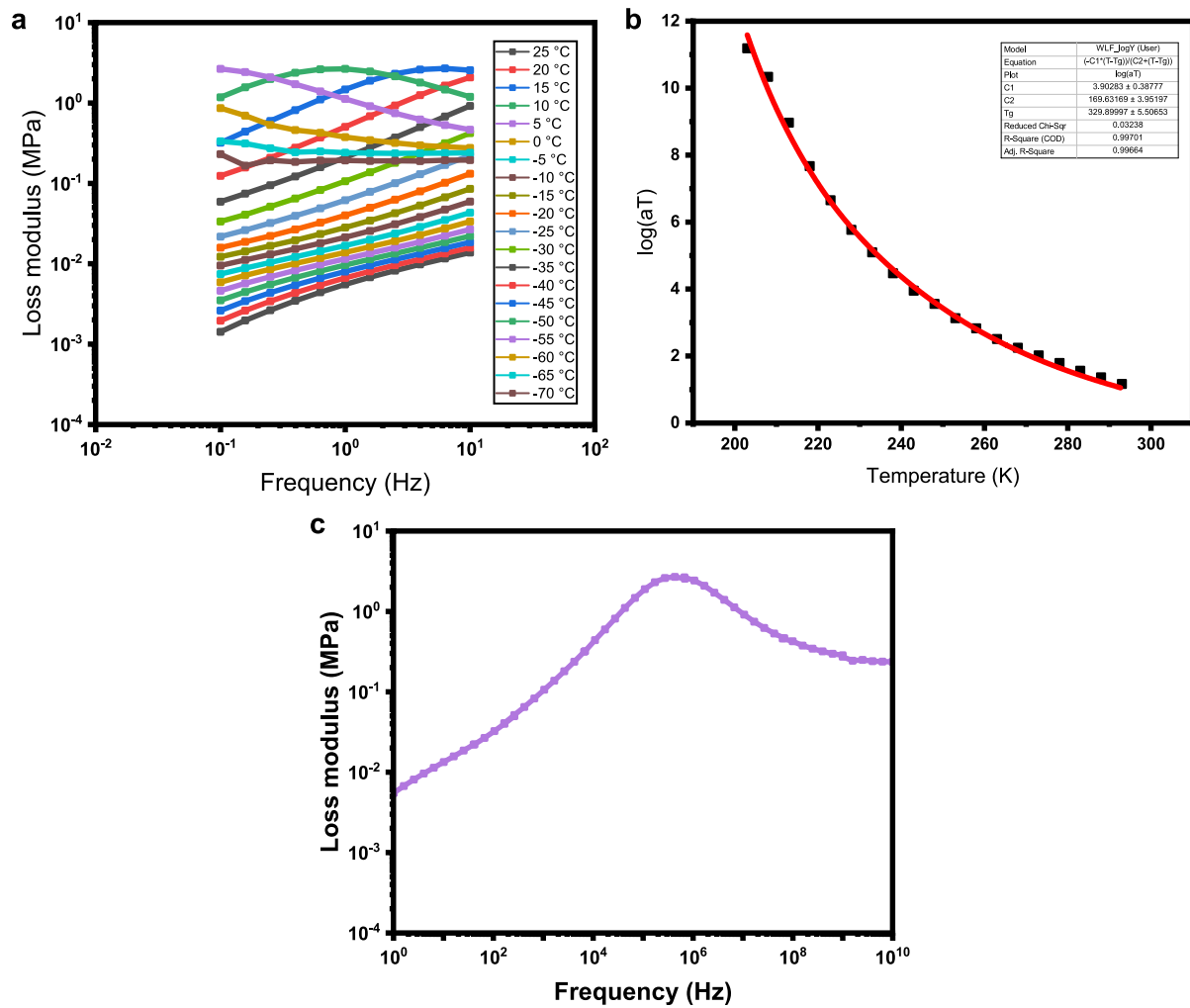


Figure S21. (a) Changes in loss modulus during a frequency sweep (0.1 – 10 Hz) at different temperatures. (b) Time-temperature superposition shift factors (a_T) for **PHA** (squares) and WLF fit of the data (red line). (c) Loss modulus master curve of **PHA** at a reference temperature of 25 °C.

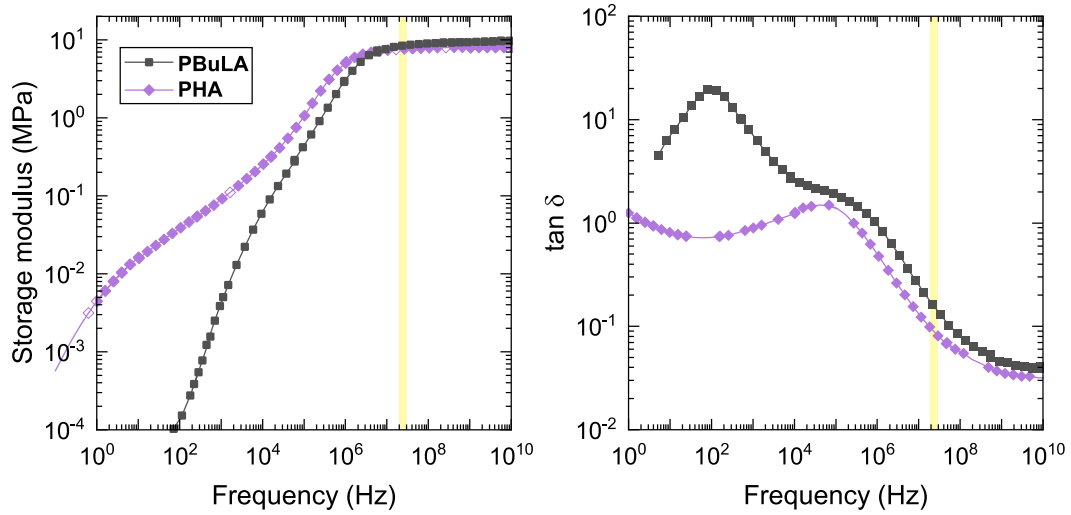


Figure S22. The time-temperature superposition of storage modulus (G') and loss modulus (G'') for **PBUuLA** (gray) and **PHA** (purple). The frequency ranges for shock wave are colored in yellow.

5.3 Comparison of high-strain stress wave dissipating abilities of **PBUuLA** and **PHA**

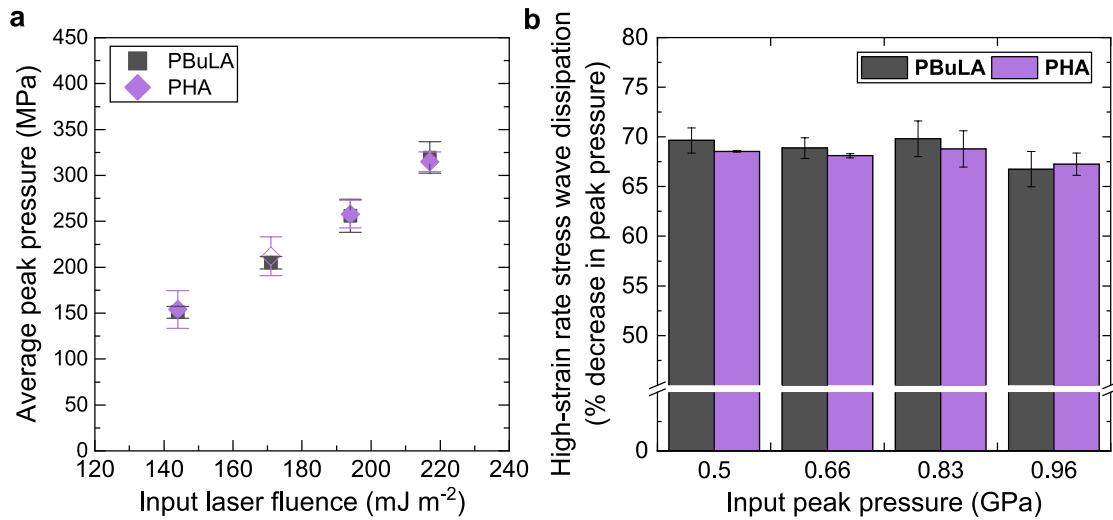


Figure S23. (a) The decrease in peak pressure as a function of input laser fluence for **PBUuLA** (gray square) and **PHA** (purple diamond) (b) The percentage of high-strain rate stress wave dissipation of **PBUuLA** (gray) and **PHA** (purple) as a function of input peak pressure.

6. Characterization of crosslinked poly(disulfide)s

6.1 Preparation method

The crosslinking density was kept 5mol% for all samples. **BuLA** (0.3 g, 1.143 mmol, 1 equiv.), **BPA-LA** (0.035 g, 0.058 mmol, 0.05 equiv.), and **BAPOs** (0.015g, 0.036 mmol, 0.03 equiv.) were added to a vial. After 0.5 ml of DCM was added into the vial, the mixture was homogeneously mixed using vortex mixing. The resulting solution was poured into a silicone mold and placed in a 60 °C oven for 2 hours. Once DCM was evaporated, the mixture was photo-cured using a white lamp (intensity ≈ 70 mW cm⁻²) for 30 minutes, resulting a slightly yellow and transparent gel (**xPBuLA-0**).

For samples containing DBU, 5 or 10wt% (relative to polymer contents) of DBU diluted in DCM was dropped onto a cross-linked polymer sample. The sample was left overnight until DBU was completely dispersed. The samples were named based on DBU content: **xPBuLA-5** and **xPBuLA-10**.

6.2 Rheological behaviors of xPBuLA system

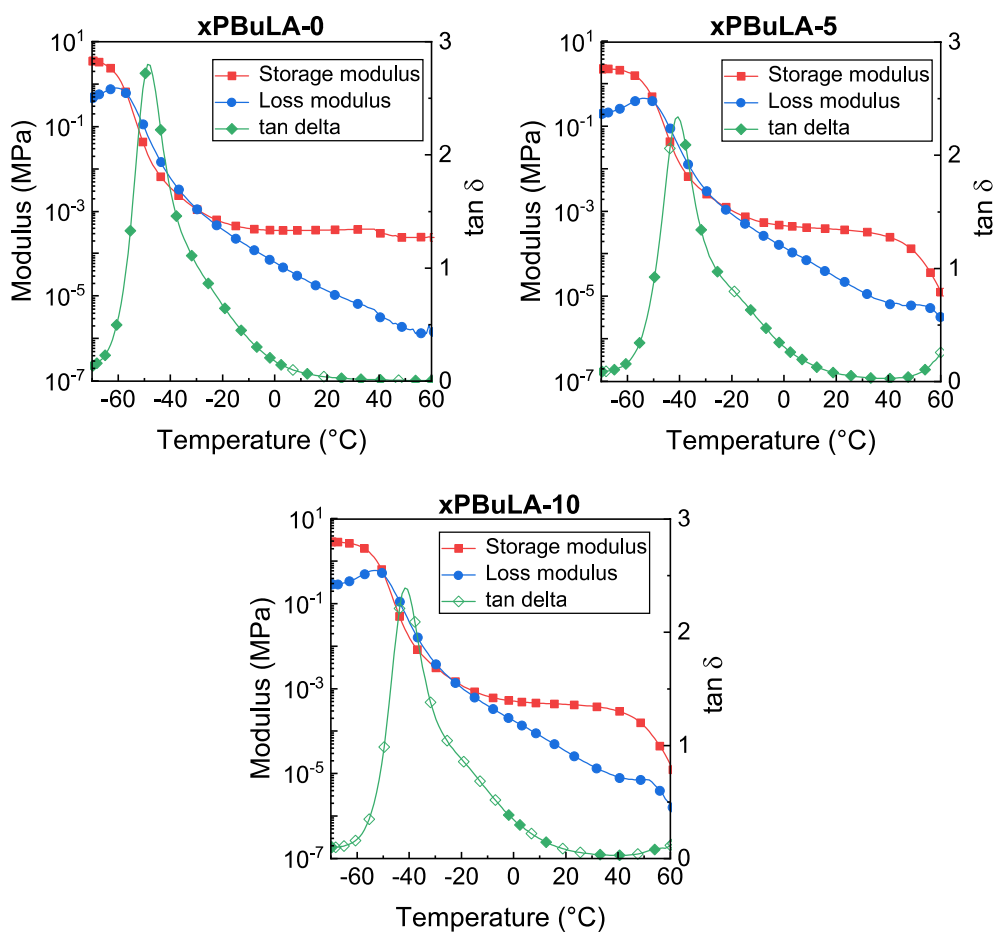


Figure S24. The change in modulus and tan δ as a function of temperature at a frequency of 1Hz for xPBuLA-0, xPBuLA-5, and xPBuLA-10.

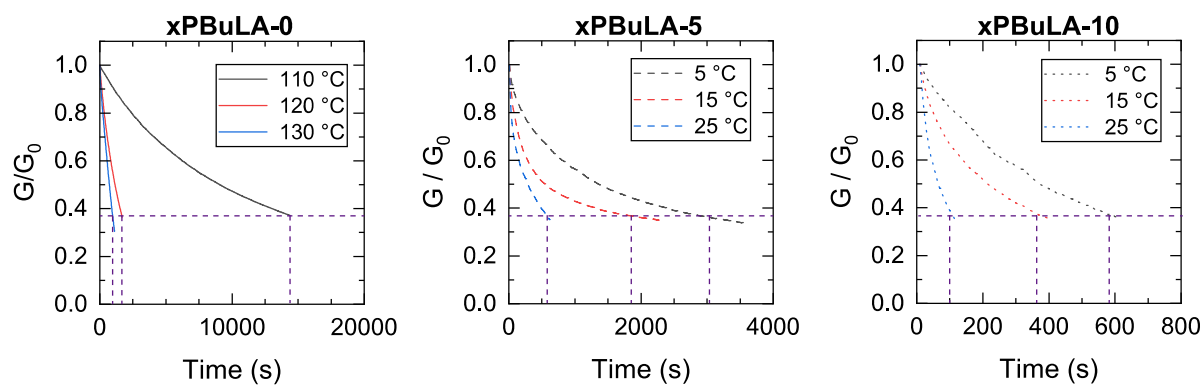


Figure S25. Normalized relaxation modulus (G/G_0) with time at constant temperatures. The relaxation times (τ^*) were defined when G/G_0 was equal to $1/e$ (dashed lines).

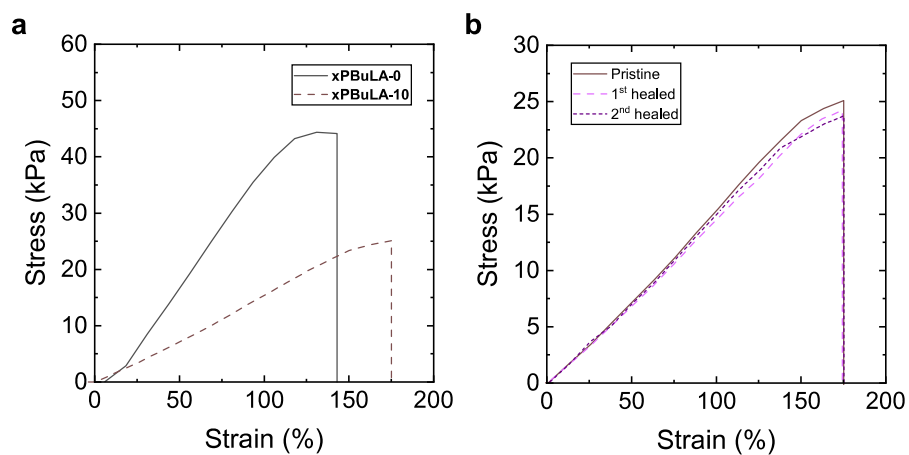


Figure S26. Representative stress and curves for (a) xPBuLA-0 and xPBuLA-10, and (b) pristine, 1st healed, and 2nd healed xPBuLA-10 samples.

6.3 Chemical recycling of xPBuLAs

Crosslinked polymers were introduced in a round-bottom flask and the flask was purged with Ar. Then, DBU solution (15 mg in 10 mL of DCM) was injected, and the mixture was stirred for 1 hour until the insoluble polymer residues disappeared. The resulting monomers and crosslinkers were separated and purified by column chromatography with 100% DCM as the eluent.

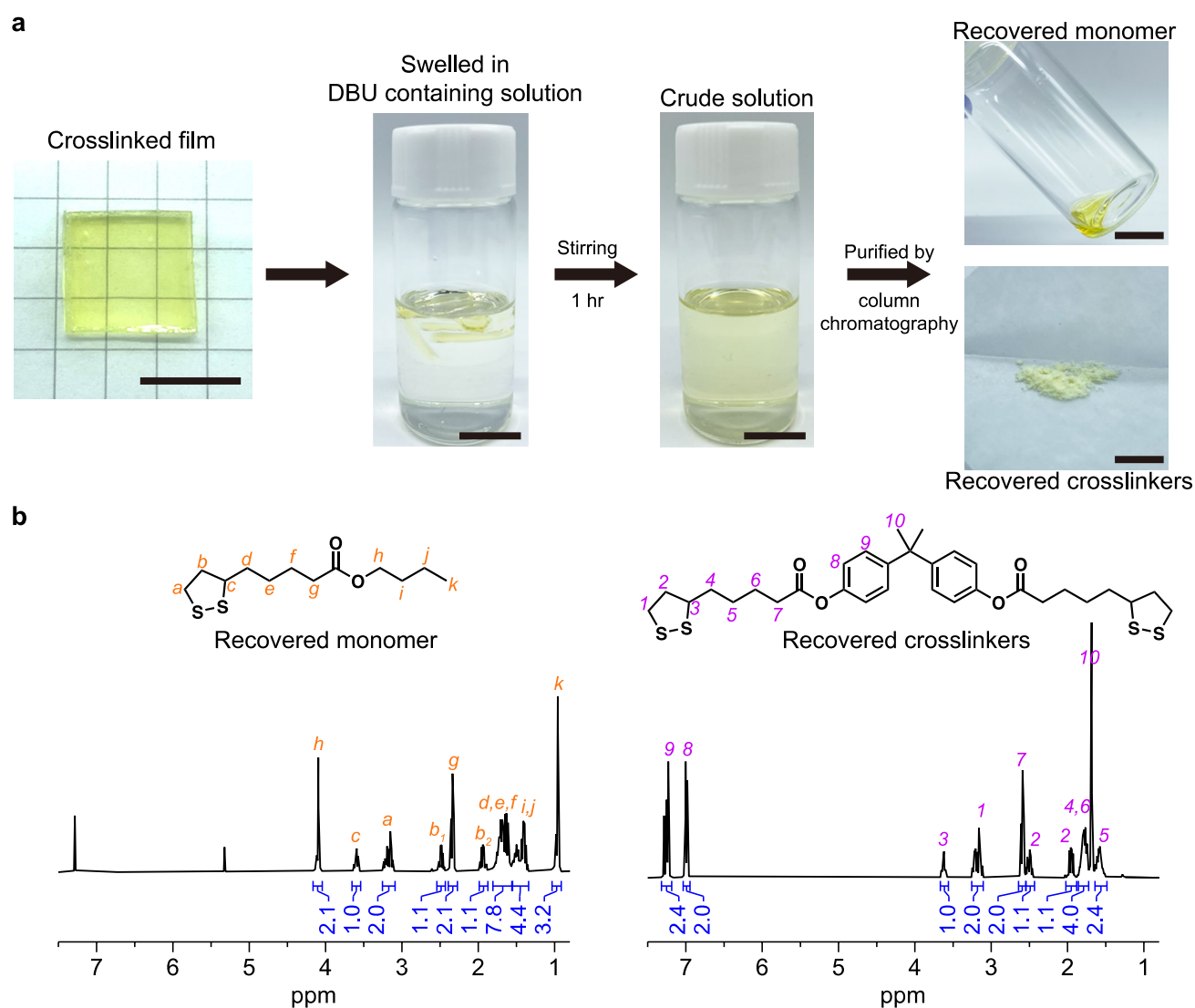


Figure S27. (a) Chemical recycling process of xPBuLAs. (b) NMR spectra of recovered monomers (BuLA) and crosslinkers (BPA-LA).

6.4 Construction of master curves for xPBuLA series

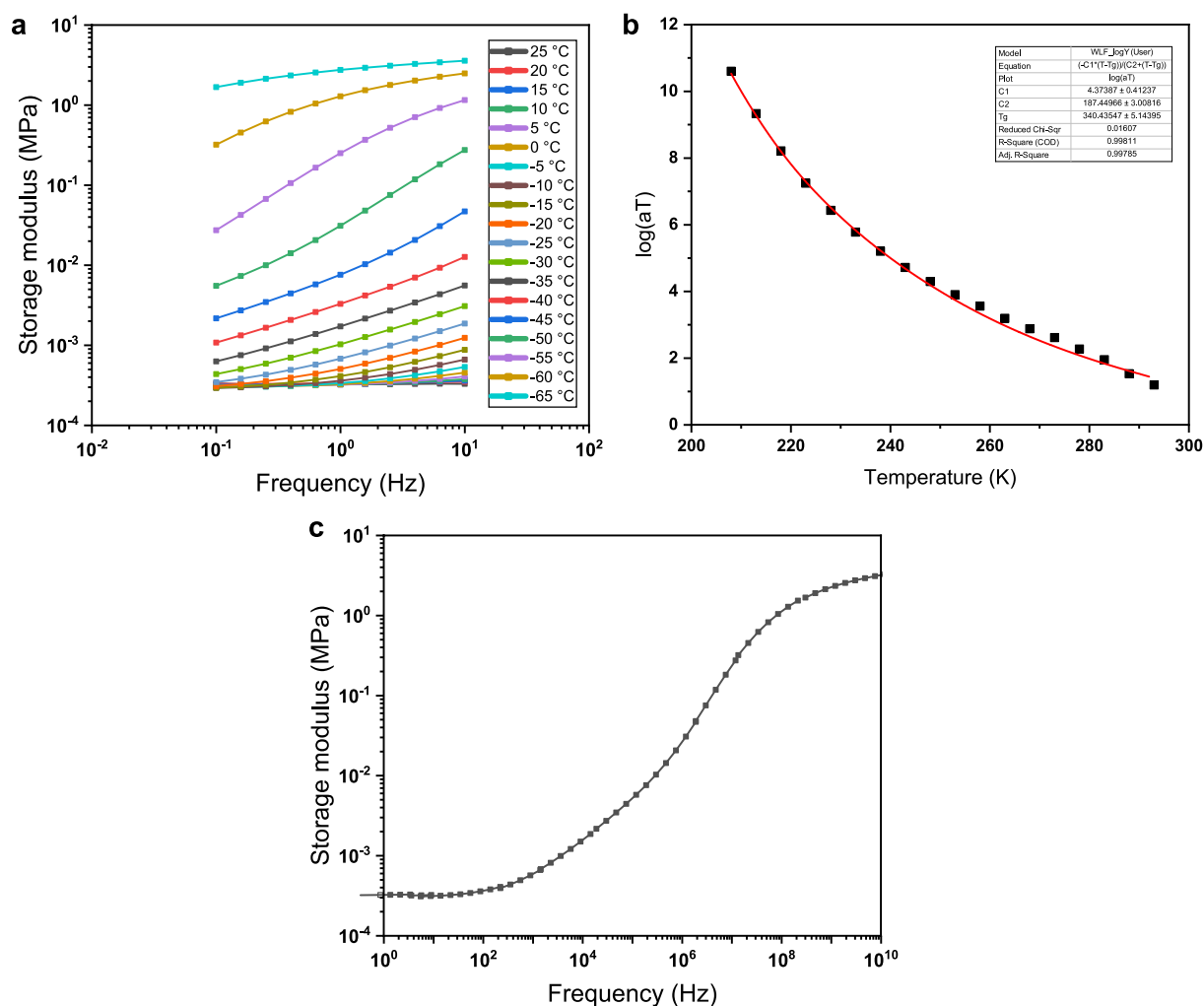


Figure S28. (a) Changes in storage modulus during a frequency sweep (0.1 – 10 Hz) at different temperatures. (b) Time-temperature superposition shift factors (a_T) for xPBuLA-0 (squares) and WLF fit of the data (red line). (c) Storage modulus master curve of xPBuLA-0 at a reference temperature of 25 °C.

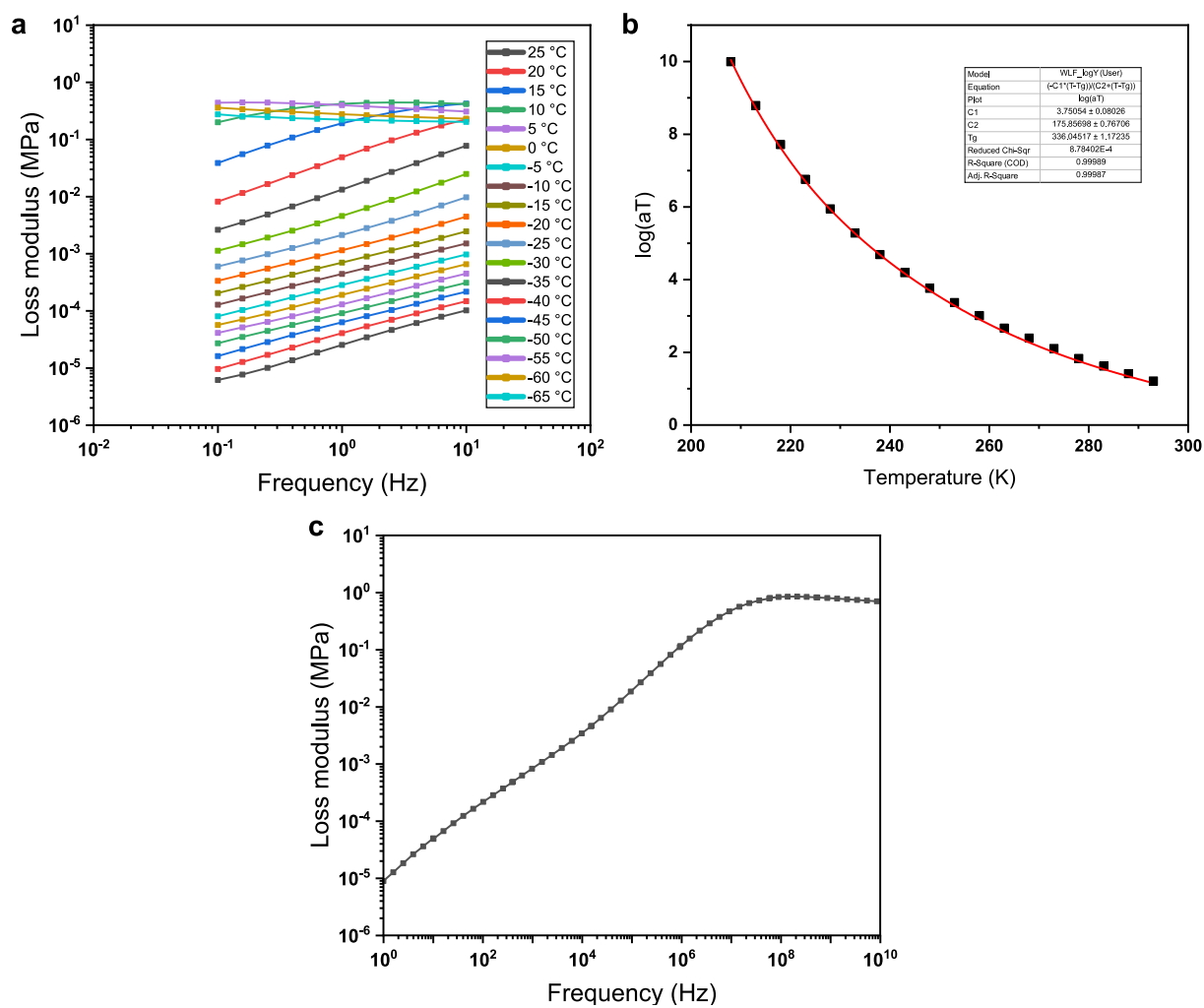


Figure S29. (a) Changes in loss modulus during a frequency sweep (0.1 – 10 Hz) at different temperatures. (b) Time-temperature superposition shift factors (a_T) for **xPBuLA-0** (squares) and WLF fit of the data (red line). (c) Loss modulus master curve of **xPBuLA-0** at a reference temperature of 25 °C.

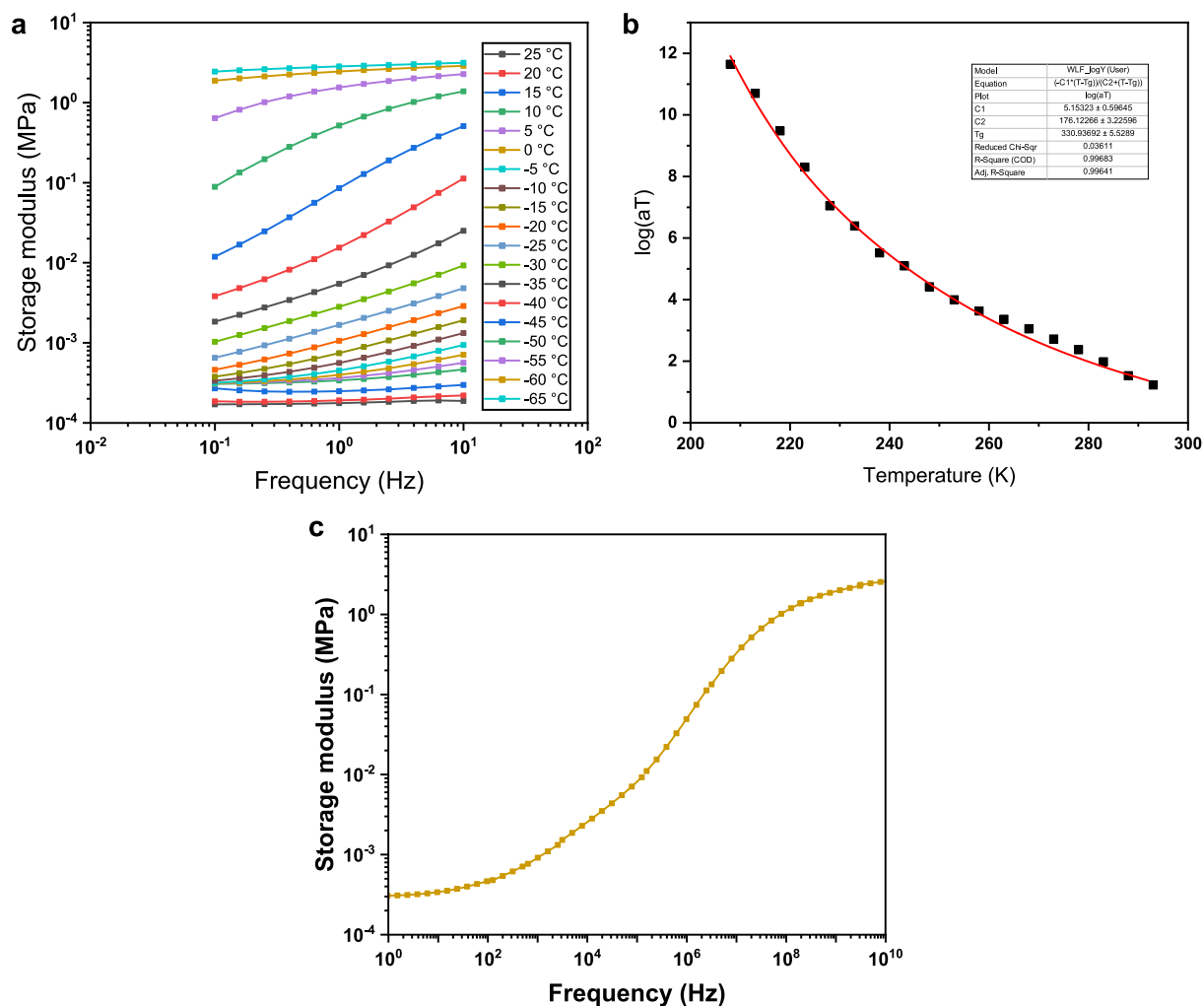


Figure S30. (a) Changes in storage modulus during a frequency sweep (0.1 – 10 Hz) at different temperatures. (b) Time-temperature superposition shift factors (a_T) for **xPBuLA-5** (squares) and WLF fit of the data (red line). (c) Storage modulus master curve of **xPBuLA-5** at a reference temperature of 25 °C.

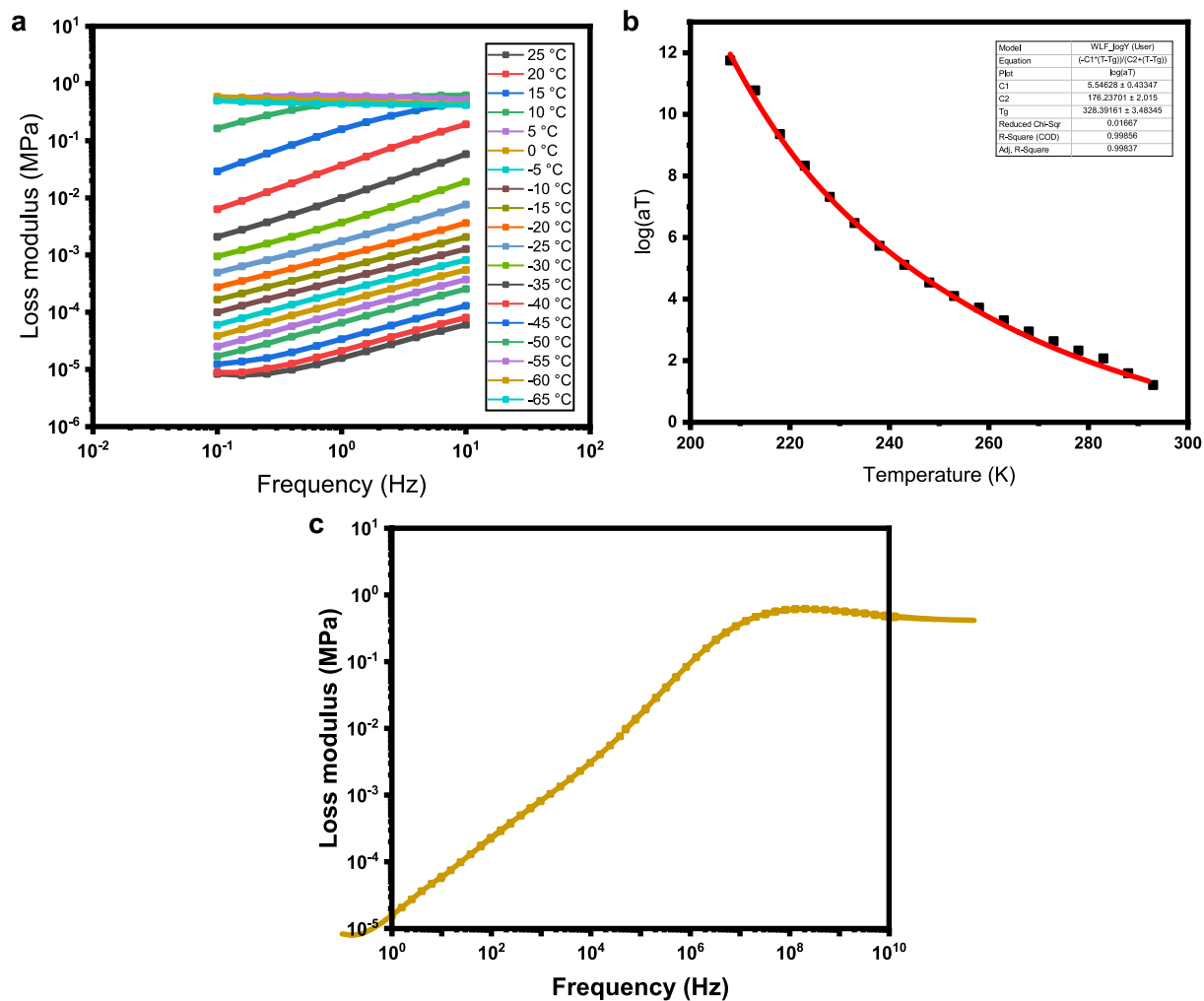


Figure S31. (a) Changes in loss modulus during a frequency sweep (0.1 – 10 Hz) at different temperatures. (b) Time-temperature superposition shift factors (a_T) for **xPBuLA-5** (squares) and WLF fit of the data (red line). (c) Loss modulus master curve of **xPBuLA-5** at a reference temperature of 25 °C.

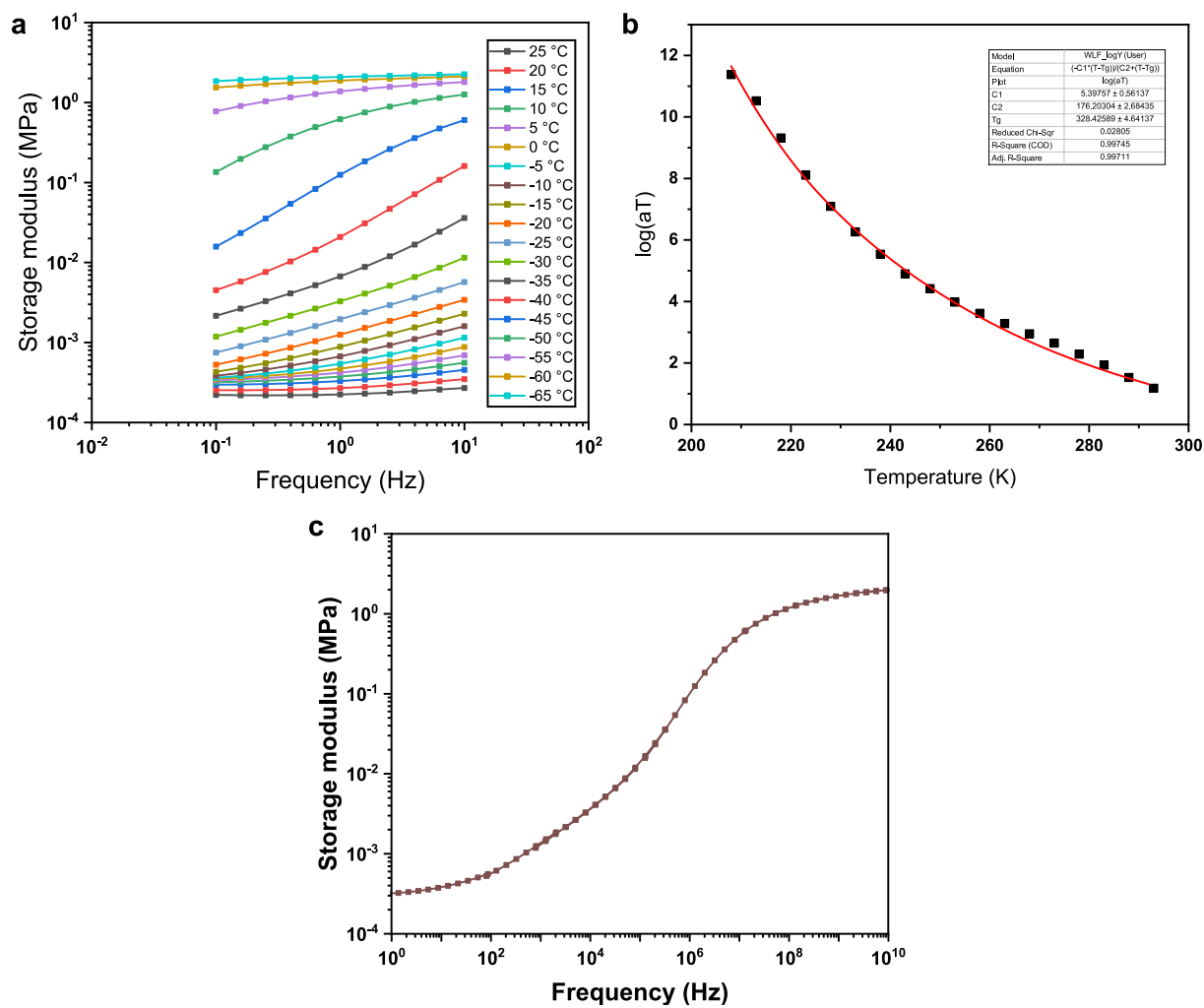


Figure S32. (a) Changes in storage modulus during a frequency sweep (0.1 – 10 Hz) at different temperatures. (b) Time-temperature superposition shift factors (a_T) for **xPBuLA-10** (squares) and WLF fit of the data (red line). (c) Storage modulus master curve of **xPBuLA-10** at a reference temperature of 25 °C.

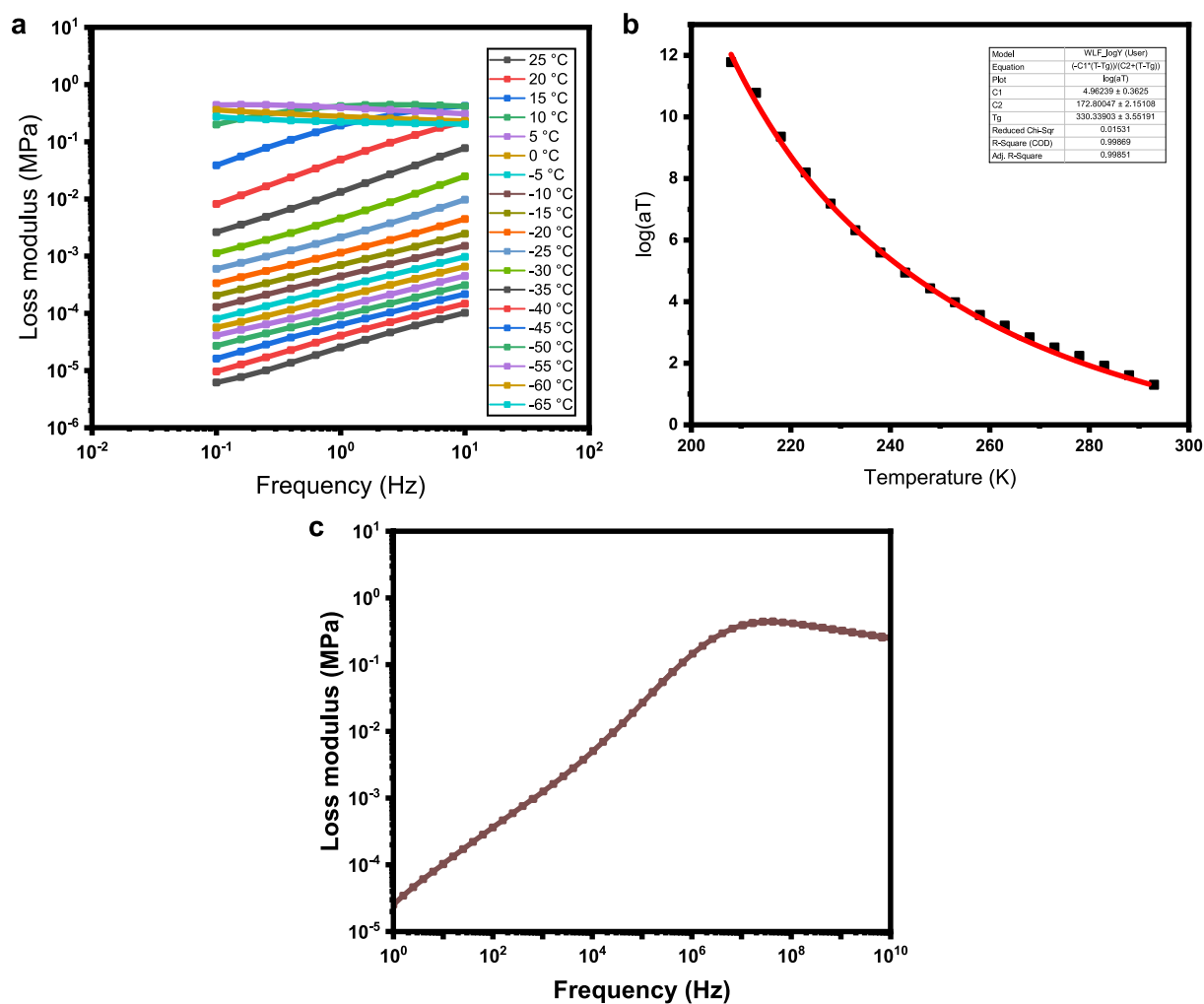


Figure S33. (a) Changes in loss modulus during a frequency sweep (0.1 – 10 Hz) at different temperatures. (b) Time-temperature superposition shift factors (a_T) for **xPBuLA-10** (squares) and WLF fit of the data (red line). (c) Loss modulus master curve of **xPBuLA-10** at a reference temperature of 25 °C.

6.5 X-ray scattering data of xPBuLA series

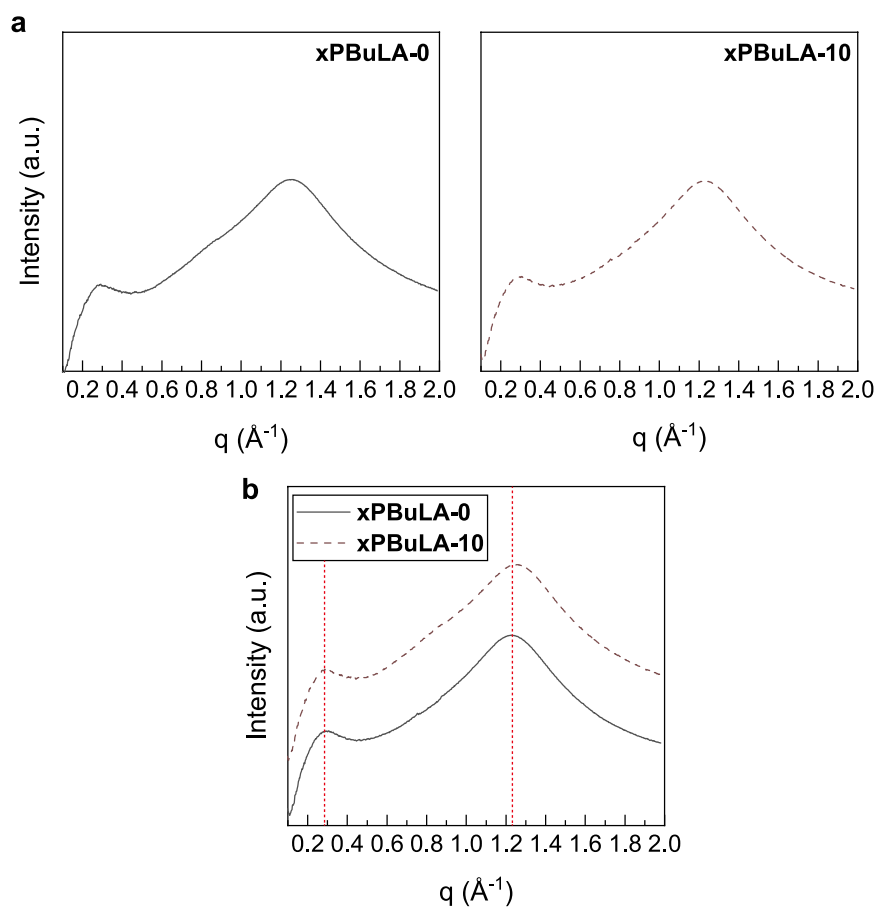


Figure S34. X-ray scattering results for xPBuLA-0 and xPBuLA-10. (a) Individual plots and (b) Overlaid plots.

6.6 Relationship between relaxation times and decrease in peak pressure

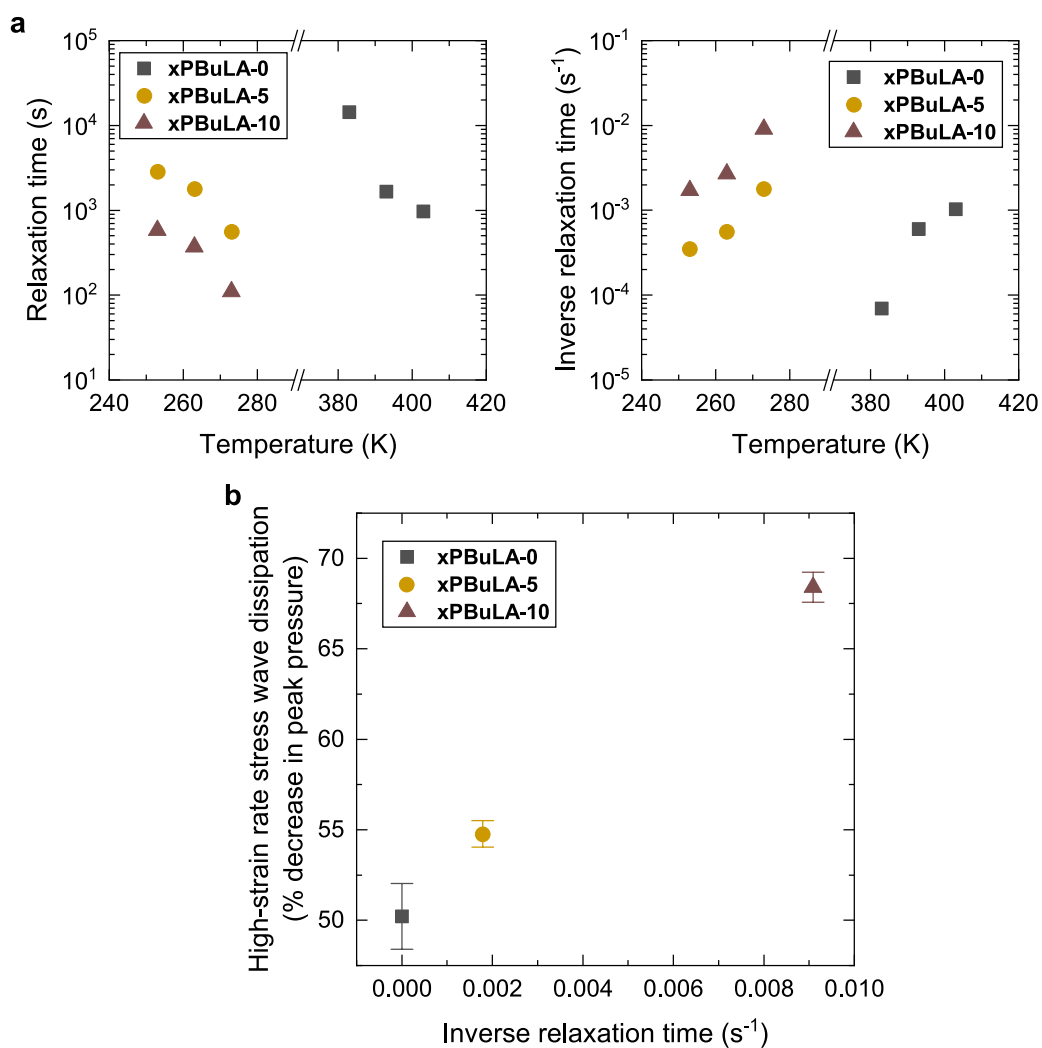
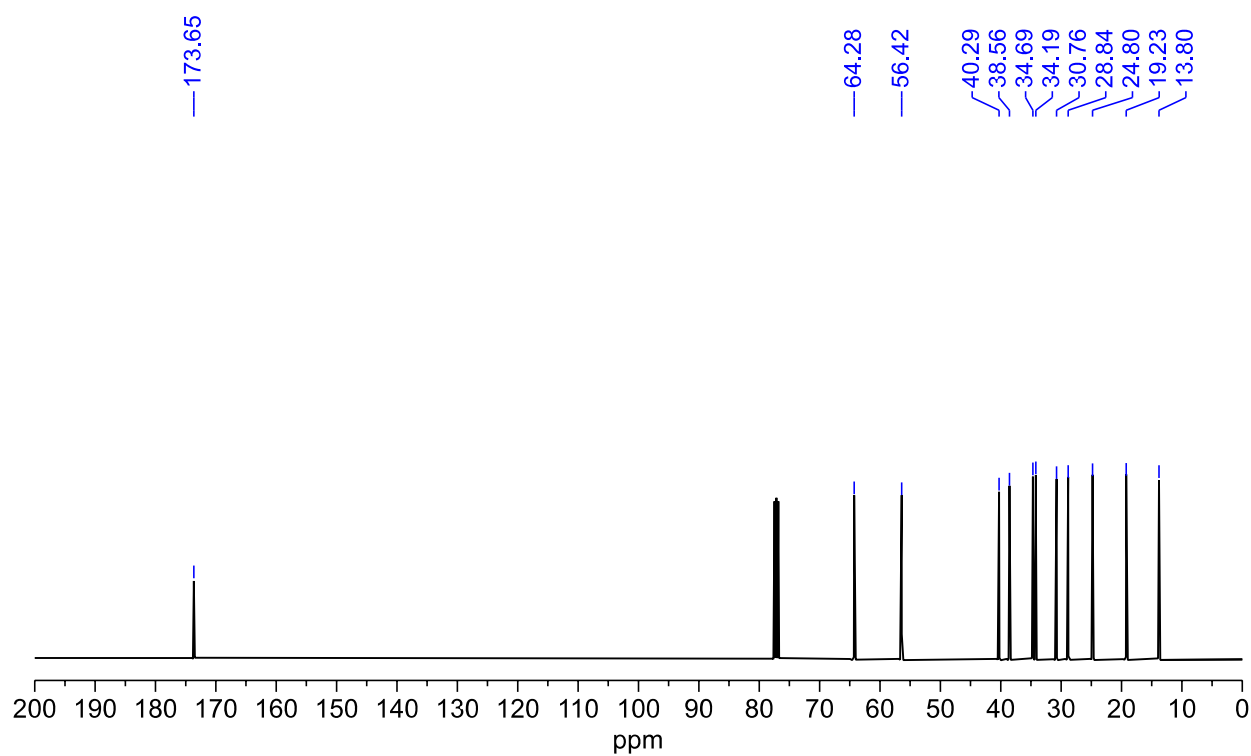
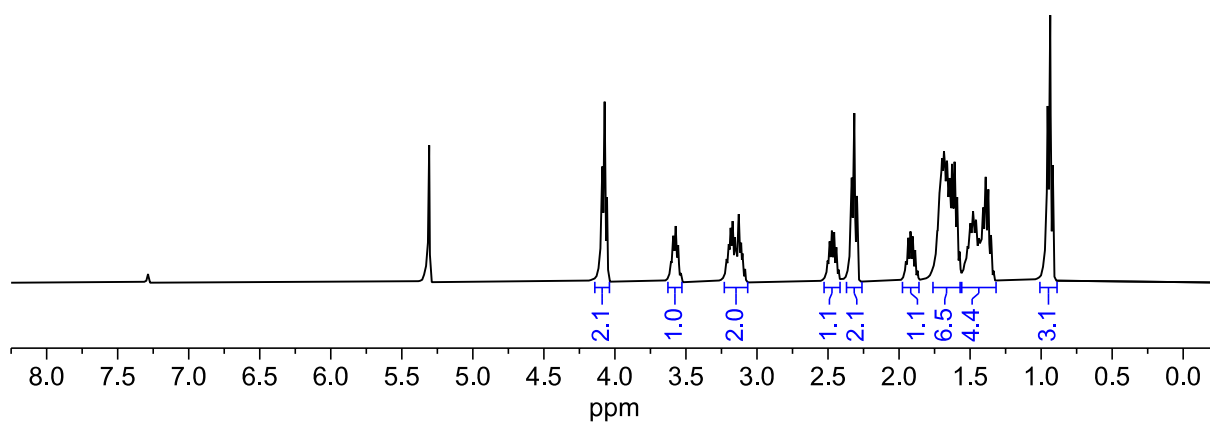
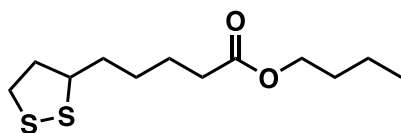


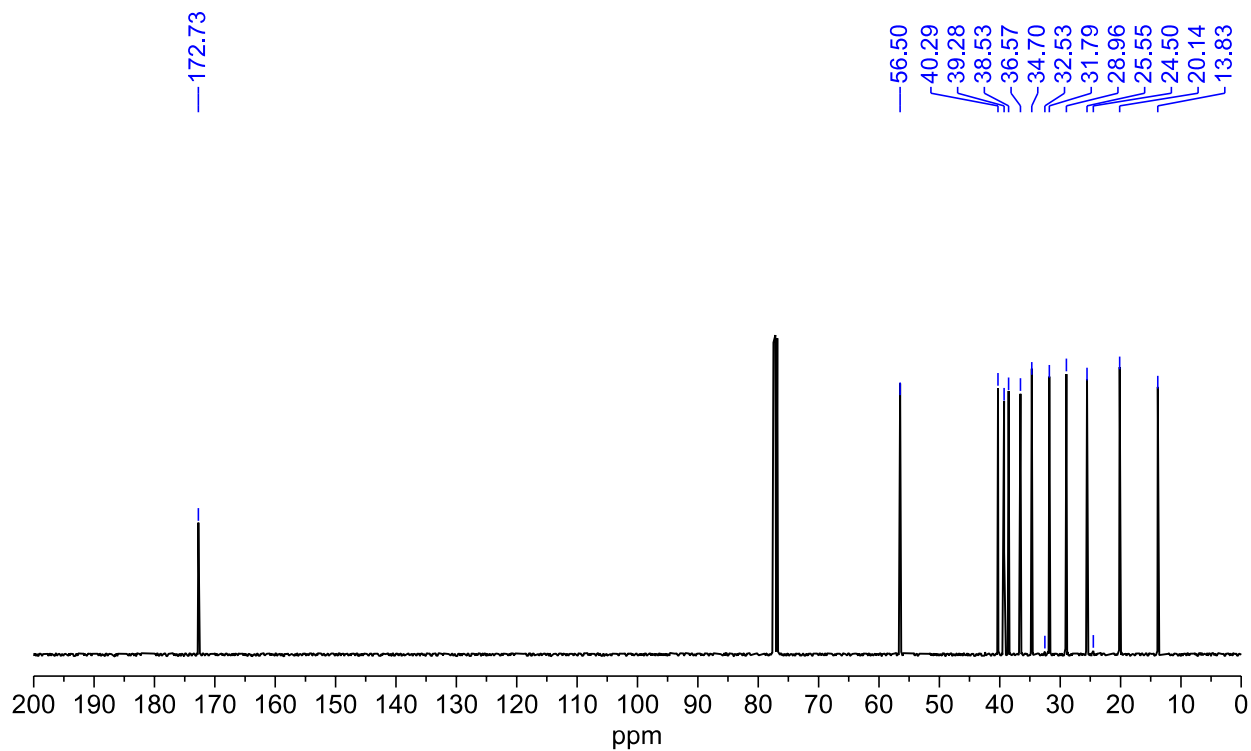
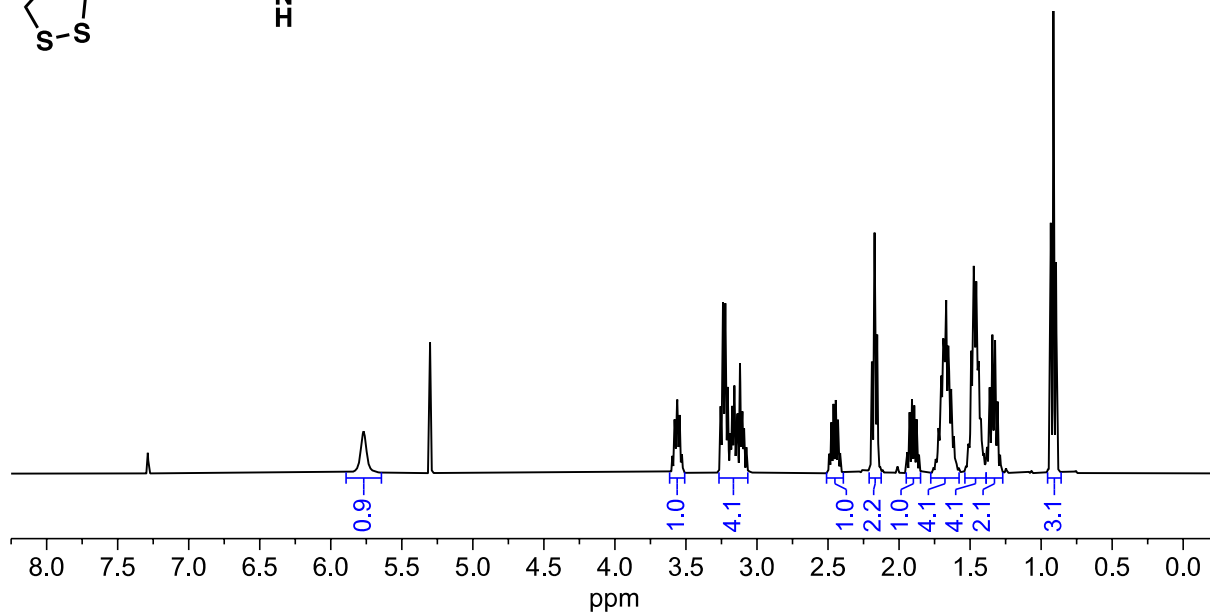
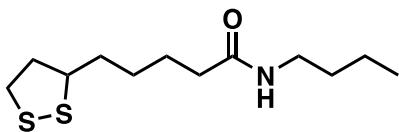
Figure S35. (a) Relaxation time and inverse relaxation time at different temperatures. (b) Relationship between inverse relaxation time and percentage decrease in peak pressure at 0.96 GPa input pressure and room temperature for xPBuLA-0, xPBuLA-5, and xPBuLA-10.

7. ^1H , ^{13}C NMR spectra of small molecules

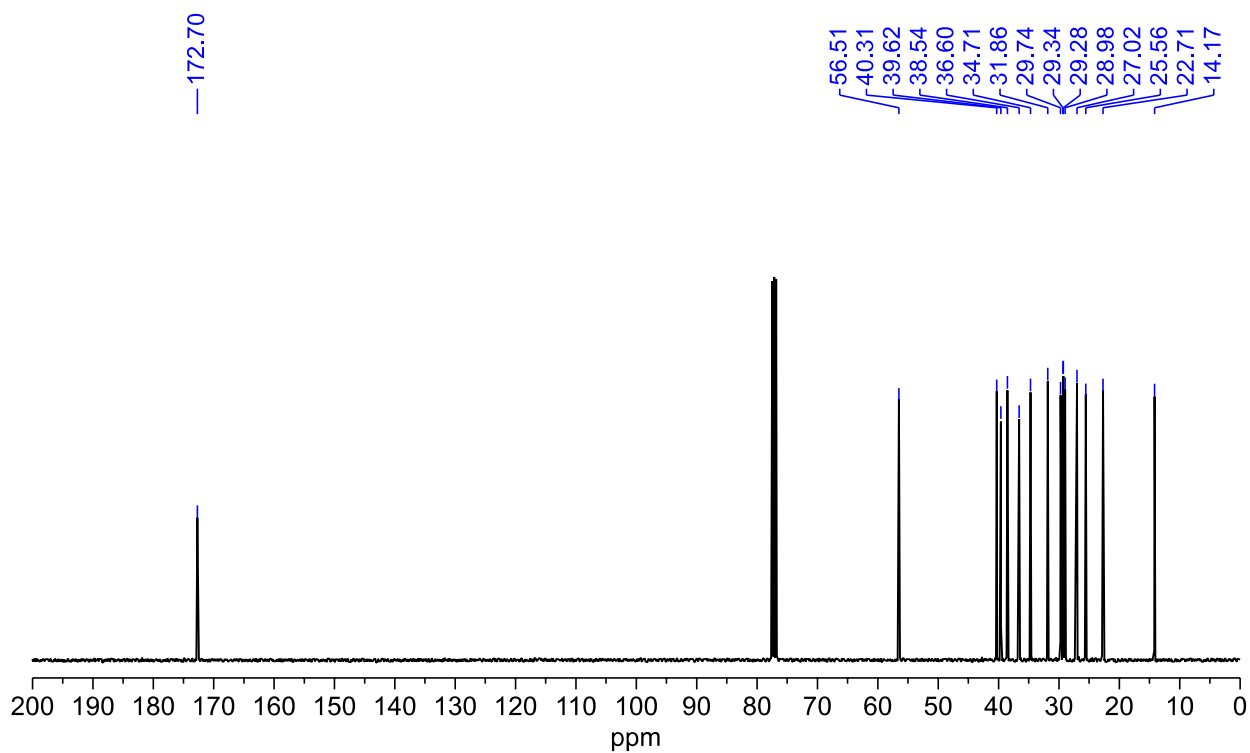
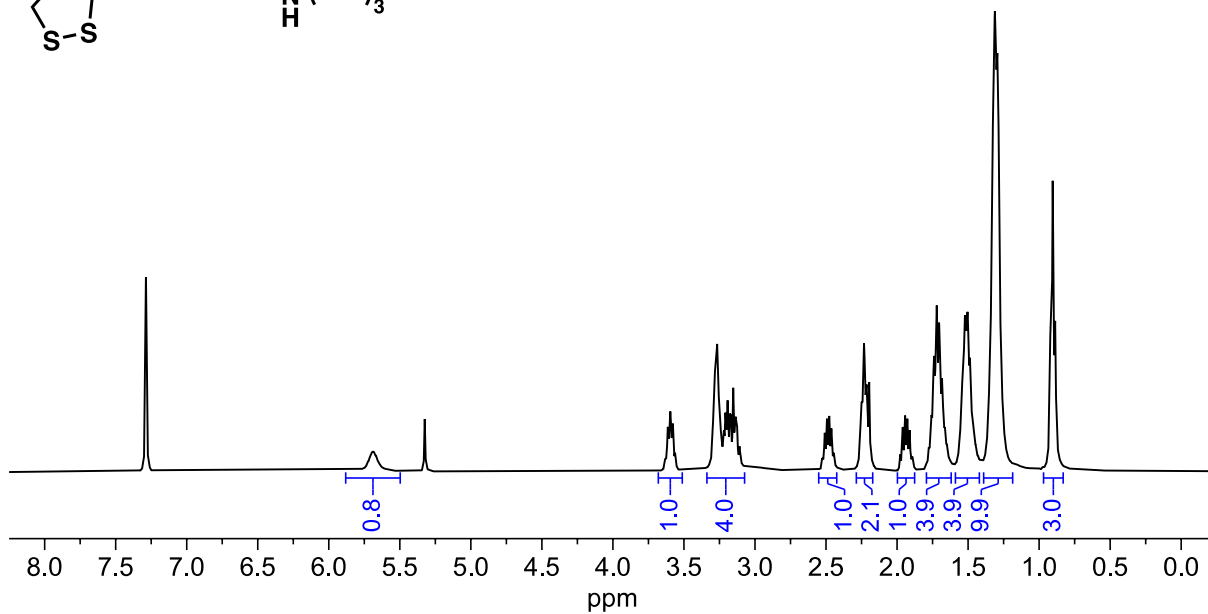
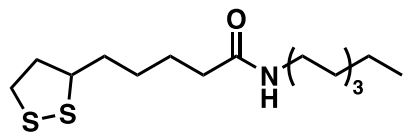
BuLA



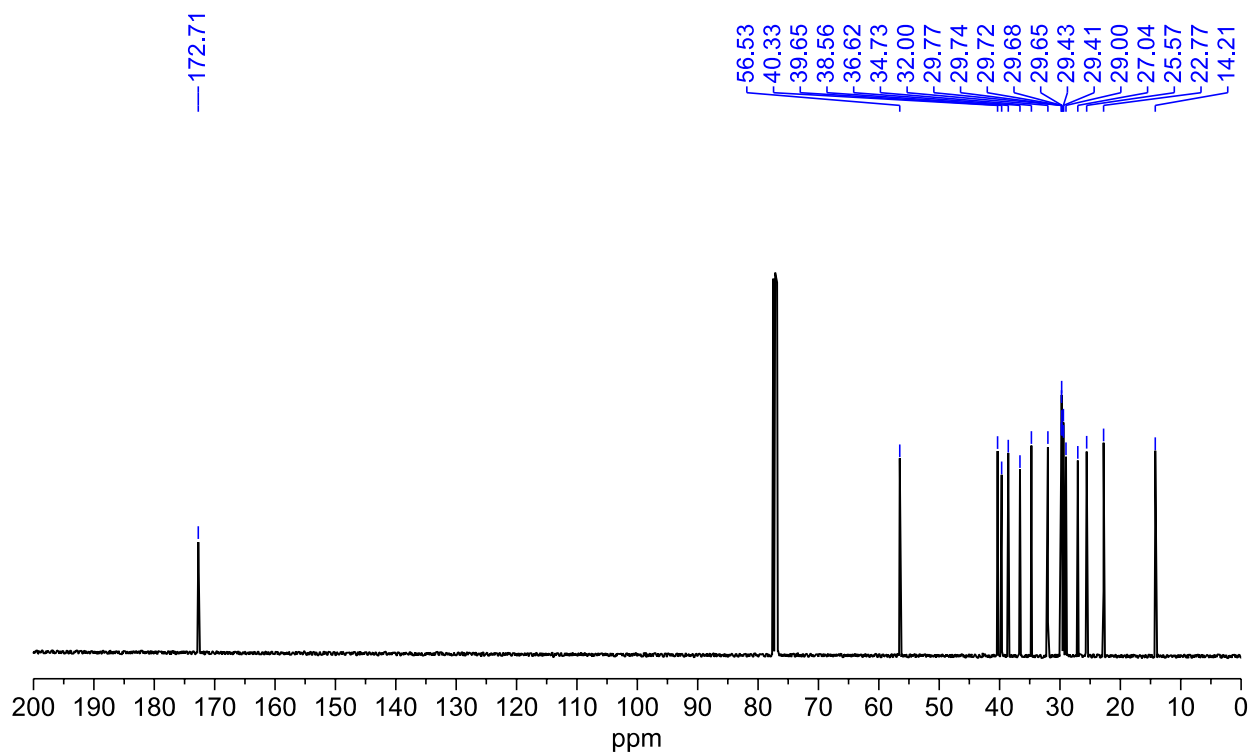
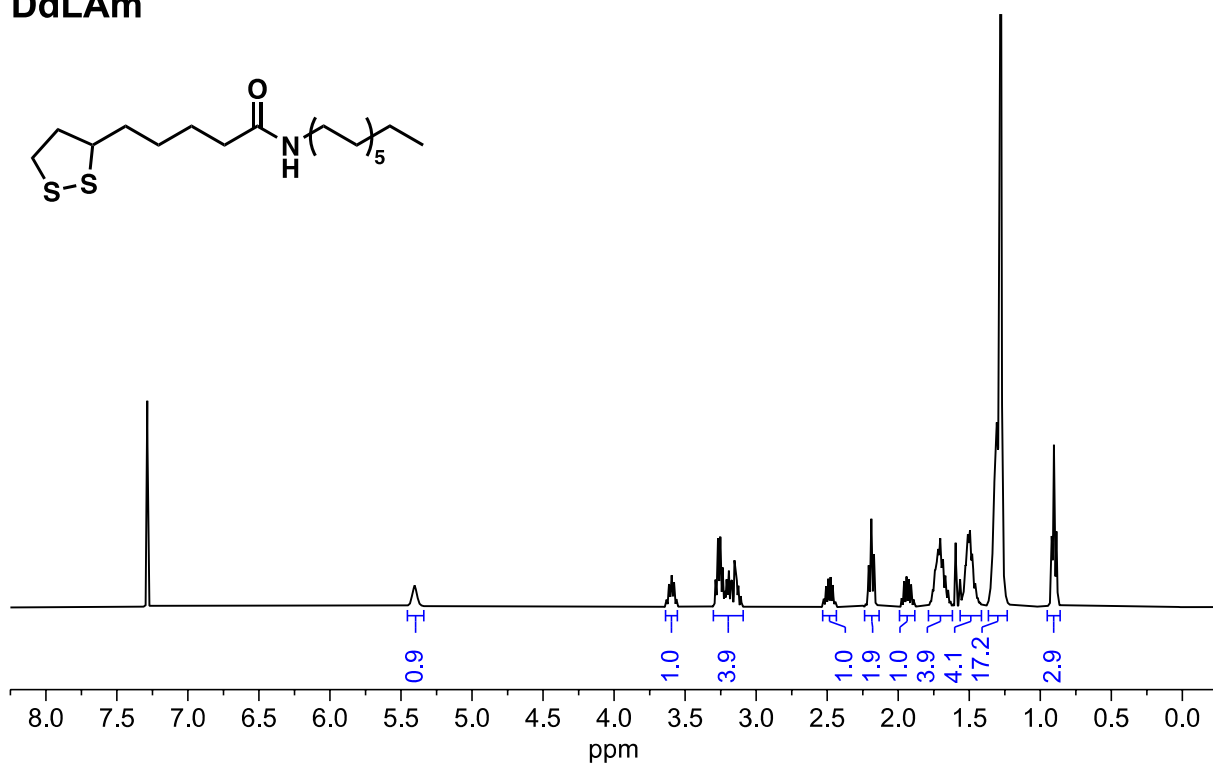
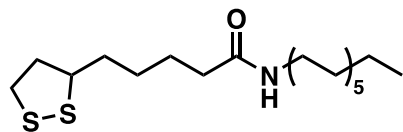
BuLAm



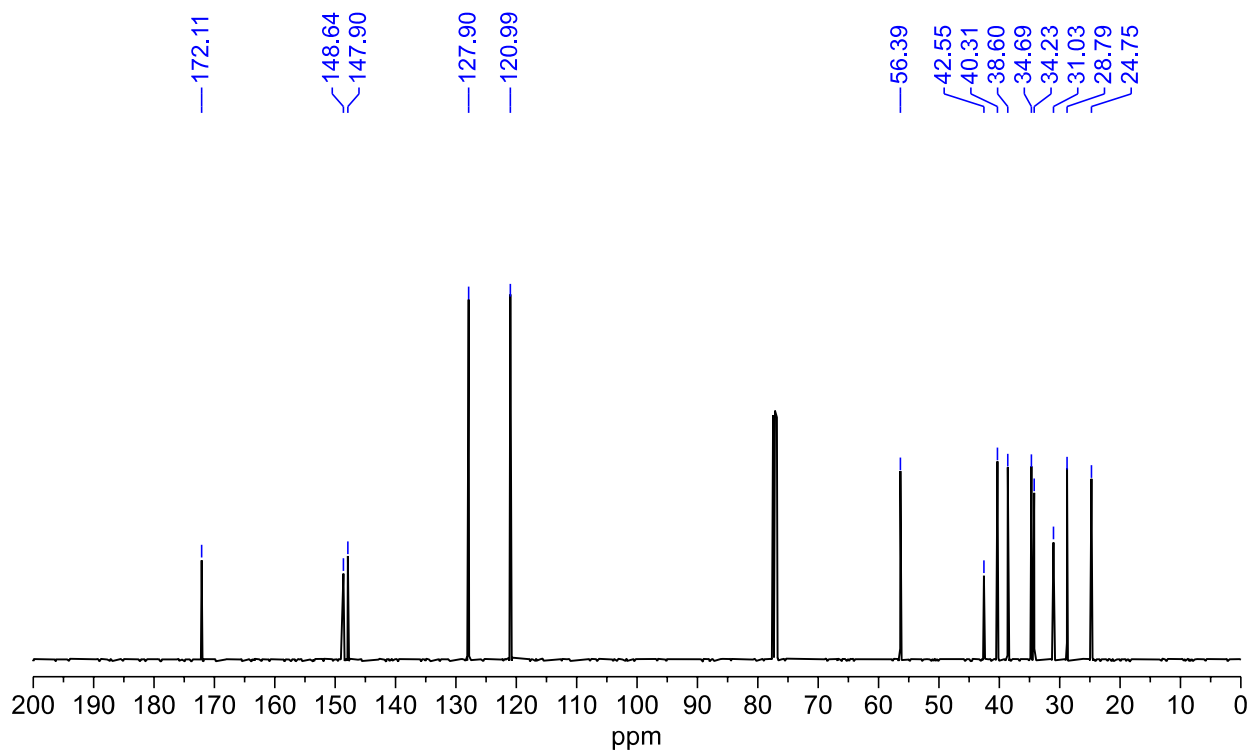
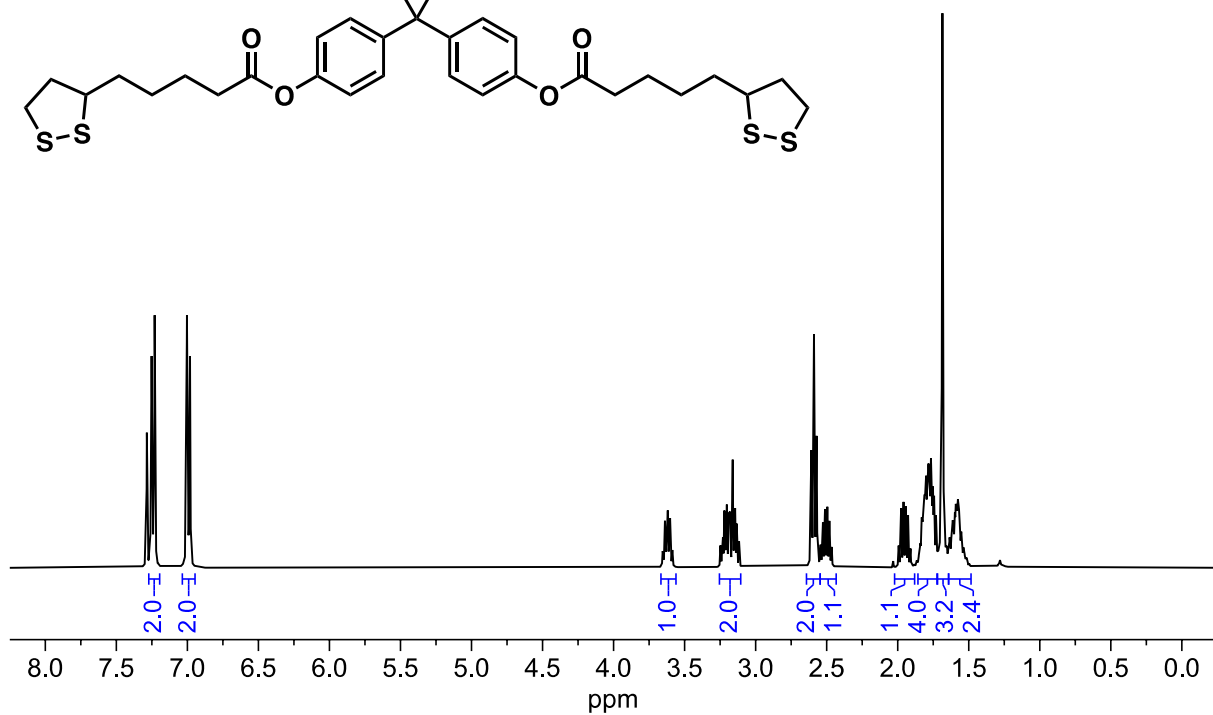
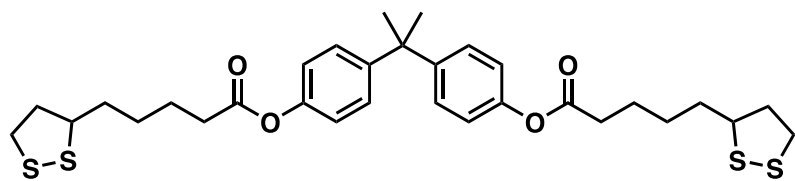
OcLAm



DdLAm



BPA-LA



8. References

- [1] K. Yang, J. Lee, N. R. Sottos, J. S. Moore, *J Am Chem Soc* **2015**, *137*, 16000–16003.
- [2] J. Wang, R. L. Weaver, N. R. Sottos, *J Appl Phys* **2003**, *93*, 9529–9536.
- [3] A. N. Pronin, V. Gupta, *J Mech Phys Solids* **1998**, *46*, 389–410.
- [4] C. S. Alexander, L. C. Chhabildas, W. D. Reinhart, D. W. Templeton, *Int J Impact Eng* **2008**, *35*, 1376–1385.